OPEN ACCESS
IOP Publishing
Journal of Physics A: Mathematical and Theoretical
J. Phys. A: Math. Theor. **58** (2025) 185002 (37pp)
https://doi.org/10.1088/1751-8121/adc9e7

First-passage statistics for Lévy flights with a drift

Amin Padash[1,*], Karol Capała[2,3], Holger Kantz[4], Bartłomiej Dybiec[5], Babak Shokri[6], Ralf Metzler[1,7,*] and Aleksei V Chechkin[1,8,9]

[1] Institute of Physics and Astronomy, University of Potsdam, 14476 Potsdam-Golm, Germany
[2] Institute of Computer Science, AGH University of Krakow, Kawiory 21, 30-059 Kraków, Poland
[3] Personal Health Data Science Group, Sano—Centre for Computational Personalised Medicine, Czarnowiejska 36, 30-054 Kraków, Poland
[4] Max Planck Institute for the Physics of Complex Systems, Nöthnitzer Str. 38, 01187 Dresden, Germany
[5] Institute of Theoretical Physics and Mark Kac Center for Complex Systems Research, Jagiellonian University, ul. St. Łojasiewicza 11, 30-348 Kraków, Poland
[6] Laser and Plasma Research Institute, Shahid Beheshti University, 19839-69411 Tehran, Iran
[7] Asia Pacific Centre for Theoretical Physics, Pohang 37673, Republic of Korea
[8] Faculty of Pure and Applied Mathematics, Hugo Steinhaus Center, Wrocław University of Science and Technology, Wyspianskiego 27, 50-370 Wrocław, Poland
[9] German-Ukrainian Core of Excellence, Max Planck Institute of Microstructure Physics, Weinberg 2, 06120 Halle (Saale), Germany

E-mail: padash1@uni-potsdam.de and rmetzler@uni-potsdam.de

Received 26 January 2025; revised 28 March 2025
Accepted for publication 7 April 2025
Published 2 May 2025

Abstract

We provide the first-passage statistics of Lévy flights in a one-dimensional semi-infinite domain, considering the effects of a constant drift μ while the jump length distribution is symmetric. By solving the space-fractional Fokker–Planck equation governing the evolution of the probability density function (PDF), we derive expressions for both the survival probability and the first-passage time for given values of the stability index α and drift parameter μ.

* Authors to whom any correspondence should be addressed.

Original Content from this work may be used under the terms of the Creative Commons Attribution 4.0 licence. Any further distribution of this work must maintain attribution to the author(s) and the title of the work, journal citation and DOI.

© 2025 The Author(s). Published by IOP Publishing Ltd

Our findings are further validated by comparing them with simulations from the stochastic Langevin equation driven by α-stable noise. Additionally, we make use of the Skorokhod theorem for processes with stationary independent increments and show that our numerical results are in good agreement with the analytical expressions for the PDF of first-passage times and survival probabilities. Specifically, in the asymptotic long-time limit, we show that for $\alpha = 2$ (Brownian motion), the first-passage time distribution follows the classical Lévy–Smirnov form and decays exponentially, irrespective of the drift direction. The survival probability exhibits a distinct asymptotic behaviour: for positive drift, it decreases exponentially, while for negative drift, it saturates to a finite value, indicating a nonzero probability for the particle to escape to $-\infty$. For $\alpha = 1$ (Cauchy process), the survival probability and the first-passage time density exhibit a power-law decay, with μ-dependent exponents. For $0 < \alpha < 1$, we find that the long-time asymptotic remains consistent with the drift-free case, but with a μ-dependent prefactor. Finally, for α-stable processes with $1 < \alpha < 2$, the first-passage time density follows a power-law decay, whose exponent depends on both α and the drift direction; concurrently, the survival probability decays in power-law form for positive drift, while in the case of negative drift, it saturates to a finite value.

Keywords: diffusion, random walks, Lévy flights, first-passage time statistics

1. Introduction

The first-passage problem as a fundamental aspect of stochastic processes arises in many physical and biological systems, and beyond [1–13]. A typical first-passage problem is to measure the probability density function (PDF) $\wp(t)$ [14], that a random process exceeds a given threshold value for the first time or escapes from a spatial domain through a prescribed boundary. The first-passage theory is an important framework to characterise the stochastic motion in a bounded domain including the flow of tracer particles through a porous medium by the advection–diffusion equation [15], diffusion-controlled reactions [16–20], non-Markovian processes [21, 22], kinetics of polymer reactions [23–26], random search processes [19, 27–30], escape from potential wells [31–33], spreading of diseases [34], nonequilibrium systems [4], renewal and nonrenewal systems [35] and polymer translocation [36, 37], among many others.

In the field of a stochastic process, there is another statistic known as first-hitting or first-arrival time, which also quantifies the efficiency of the spatial exploration and search properties of the process. The first-hitting time corresponds to the event when a specific point-like or finite size target is visited for the first time [38–41]. Once the random walker crosses the target, the statistic of the distance beyond the target ('leapovers') is also of interest [42–45].

Lévy flights are Markovian random walk processes in which the distribution of jump lengths are drawn from an α-stable long-tailed distribution with power-law asymptote [46–48]. The broad distribution of occasional, extremely long jumps effects the diverging variance of the process [49, 50]. Lévy flights with their features, independent stationarity increments or self-similarity, have accordingly turned out to apply to the statistical description of scale-invariant phenomena in diverse complex dynamic processes [46, 51–53]. To name a few, we mention human movement distributions [12, 54, 55], animal foraging patterns [56], diffusive transport of light [57], tracer motion in living cells [58–61], heat transport in magnetised plasmas [62, 63] and Lévy statistics in stock market price fluctuations [64–66].

In the literature, there are several results regarding the first-passage time statistics for Lévy flights in discrete and continuous-time in semi-infinite intervals [42, 43, 67–74]. Adding a constant drift even in the simplest random walk problem such as the Brownian motion, give rise to new features. In the case of Brownian motion the first-passage time PDF $\wp(t)$, in the presence of a constant drift, asymptotically decays exponentially in time [2]. It is worth noting that Brownian motion with a drift applies to describe the effect of linear trends in the statistics of records [75, 76] whose relation to the first-passage theory is well known [2, 4] and has specific applications to finance [77–79].

Another relevant example are diffusion processes with heavy-tailed jump length distribution in the presence of a constant drift, in which the theoretical aspects of the first-passage statistics become more challenging. In this case, extensions were made to the extreme values statistics of stochastic processes with a constant drift for symmetric Lévy flights by means of record-breaking statistics [75, 78, 80]. The statistics of records of a one-dimensional discrete random walk in the presence of a constant bias was studied [75], and the effect of a linear drift on the record statistics of a Gaussian random walk was considered [78]. Moreover, in [80] the asymptotic of the expected maximum of discrete Lévy flights with a drift on a line was investigated. We also note that, with the help of record statistics, the 'time since maximum' or 'drawdown time' of the general class of Lévy processes (processes with stationary, independent increments) with drift were studied [81]. We finally mention the classical results regarding α-stable processes with a drift. A limit distribution for the first-passage time of random walks with a drift which were shown to belong to the domain of attraction of α-stable laws [82], and explicit information about the potential kernel and hitting times of α-stable processes with a drift was obtained [83], as well as an asymptotic expansion of the hitting times of α-stable process in d-dimension with a drift derived [84].

Following the results in [73], we here provide the first-passage statistics for symmetric Lévy flights with a drift in a semi-infinite interval. By employing the Skorokhod theorem [85, 86], which provides an analytical expression for the first-passage time PDF of random processes with stationary independent increments (Lévy processes) in a semi-infinite interval, we demonstrate analytic results in certain special cases of the α-stable probability laws. Furthermore, with two numerical approaches based on the space-fractional Fokker–Planck equation and the Langevin equation, the survival probability and the first-passage time PDF for different values of the stability index α and the drift parameter μ is obtained.

The paper is organised as follows. In section 2, we introduce the Skorokhod theorem in a semi-infinite interval and explore its relationship with the first-passage time and survival probability. Moving on to section 3, we define the space-fractional Fokker–Planck equation based on the characteristic function of an α-stable random process under the influence of a drift. In this section, we also provide the corresponding Langevin equation for Lévy flights with a drift. The subsequent sections 4 through 8 are dedicated to presenting numerical results for the survival probability and the first-passage time PDF for symmetric α-stable distributions. These numerical findings are compared with the analytical results derived using the Skorokhod theorem. Finally, in section 9, we conclude the paper by summarising our key findings and their broader implications. The appendices contain detailed descriptions of our numerical models for the fractional advection-diffusion equation, as well as the derivations of the first-passage time and survival probability.

Figure 1. Schematic of our setup. We consider a semi-infinite interval $(-\infty, d]$. The initial condition is represented by a δ-distribution located at $x(0) = 0$.

2. First-passage statistics and the Skorokhod theorem

The first-passage time PDF $\wp(t)$ is defined as the negative time derivative of the survival probability $S(t)$ (sometimes called the persistence probability) [2, 3],

$$\wp(t) = -\frac{\mathrm{d}S(t)}{\mathrm{d}t}, \tag{1}$$

which refers to the probability that up to time t the stochastic process stays within the domain. In the Laplace domain with initial condition $S(0) = 1$ the relation between the survival probability and the first-passage time reads

$$\wp(\lambda) = 1 - \lambda S(\lambda). \tag{2}$$

From an analytical point of view, the Skorokhod theorem provides a general formula for the first-passage time PDF in the Laplace domain for a broad class of Lévy processes [85, 86]. For the setup shown in figure 1 in which the process starts at $x = 0$ and is limited to move in the semi-infinite interval $(-\infty, d]$, reads

$$\wp(\lambda) = \langle \mathrm{e}^{-\lambda t} \rangle = \int_0^\infty \mathrm{e}^{-\lambda t} \wp(t)\, \mathrm{d}t = 1 - p_+(\lambda, d), \tag{3}$$

where the auxiliary measure $p_+(\lambda, x)$ is defined via its Fourier transform as

$$\begin{aligned} q_+(\lambda, k) &= \int_{-\infty}^{\infty} \mathrm{e}^{\mathrm{i}kx} \frac{\partial p_+(\lambda, x)}{\partial x} \mathrm{d}x \\ &= \exp\left(\int_0^\infty \frac{\mathrm{e}^{-\lambda t}}{t} \int_0^\infty \left(\mathrm{e}^{\mathrm{i}kx} - 1\right) P_\alpha(x, t)\, \mathrm{d}x \mathrm{d}t \right). \end{aligned} \tag{4}$$

Here the function $P_\alpha(x, t)$ is the PDF of the process. The boundary condition reads $p_+(\lambda, x) = 0$ at $x \leqslant 0$. For convenience in analytical calculations we write equation (4) in the following form,

$$\frac{\partial}{\partial \lambda} \ln q_+(\lambda, k) = \int_0^\infty \mathrm{e}^{-\lambda t} \int_0^\infty \left(1 - \mathrm{e}^{\mathrm{i}kx}\right) P_\alpha(x, t)\, \mathrm{d}x \mathrm{d}t. \tag{5}$$

In the following section, we define the two numerical methods employed for comparison with our results derived from the Skorokhod theorem for the first-passage time PDF and the survival probability.

3. Numerical tools

3.1. Space-fractional Fokker–Planck equation

A space-fractional Fokker–Planck equation is a deterministic equation for the PDF $P_\alpha(x,t)$, also known as the Smoluchowski equation or the Kolmogorov forward equation, given by [14, 87]

$$\frac{\partial}{\partial t}P_\alpha(x,t)+\mu\frac{\partial}{\partial x}P_\alpha(x,t)=K_\alpha\frac{\partial^\alpha}{\partial|x|^\alpha}P_\alpha(x,t), \tag{6}$$

where the initial condition is $P_\alpha(x,0)=\delta(x)$, and the space-fractional derivative operator $\partial^\alpha/\partial|x|^\alpha$ is defined in terms of its Fourier transform, $\int_{-\infty}^{\infty}\mathrm{e}^{\mathrm{i}kx}[\partial^\alpha/\partial|x|^\alpha]f(x)\mathrm{d}x=-|k|^\alpha f(k)$, and where $f(k)=\int_{-\infty}^{\infty}\mathrm{e}^{\mathrm{i}kx}f(x)\mathrm{d}x$ is the Fourier transform of $f(x)$. In equation (6), the stability (Lévy) index α is in the range $0<\alpha\leqslant 2$, the scale parameter (generalised diffusion coefficient) is positive ($K_\alpha>0$) and the drift parameter μ accounting for the constant drift in the system is any real number. By applying the Fourier transform to the left-hand side of equation (6), it can be readily shown that

$$P_\alpha(k,t)=\int_{-\infty}^{\infty}\mathrm{e}^{\mathrm{i}kx}P_\alpha(x,t)\,\mathrm{d}x=\exp\left(-tK_\alpha|k|^\alpha+\mathrm{i}k\mu t\right), \tag{7}$$

which represents the characteristic function of an α-stable PDF [85, 88]. This result stems from the limiting distributions of sums of independent, identically distributed (i.i.d.) random variables [51, 89], as described by the generalised central limit theorem [47, 48, 90]. The numerical scheme used to solve equation (6) is detailed in appendix A. For the numerical simulations based on the space-fractional diffusion equation, an additional absorbing boundary was imposed on the left-hand side of the initial position of the random walker, placed at a significant distance away to resemble a semi-infinite interval. Specifically, in our simulations, each random walker begins at $x(0)=0$, with absorbing boundaries set at $x=d=0.5$ and $x=-2000$. In this paper, we utilise the Skorokhod theorem to explore the first-passage statistics of α-stable probability laws in the presence of a constant drift. The behaviour of these statistics varies depending on the sign of the drift μ and the value of the stability index α. We begin by deriving $\wp(t)$ for Brownian motion with a drift, followed by an analysis of the symmetric Cauchy law ($\alpha=1$). We then examine α-stable processes with $0<\alpha<1$ and conclude with the study of α-stable processes where $1<\alpha<2$, all under the influence of a constant drift.

3.2. Comparison with α-stable distributions

To evaluate the performance of the numerical scheme used to solve the space-fractional advection-diffusion equation, we compare the numerical results to the theoretical predictions for the shapes of α-stable PDFs in the presence of a drift. For computational purposes, it is advantageous to perform the inverse Fourier transform of the characteristic function in the M-form, as outlined in [90]. By employing the method described in [91] and converting the distribution's parameters from the M-form to the standard form as discussed in [73], we demonstrate that the numerical results are in excellent agreement with the theoretical expectations.

The interval is confined to $[-L,L]$, with the initial condition represented by a Dirac δ-function centred at the middle of the domain, where $L=20$ ($x(0)=0$). Absorbing boundary conditions are applied at the boundaries. The PDF for various combinations of the stability index α and the drift parameter μ at $t=1$ is shown in figure 2. Across all cases and throughout

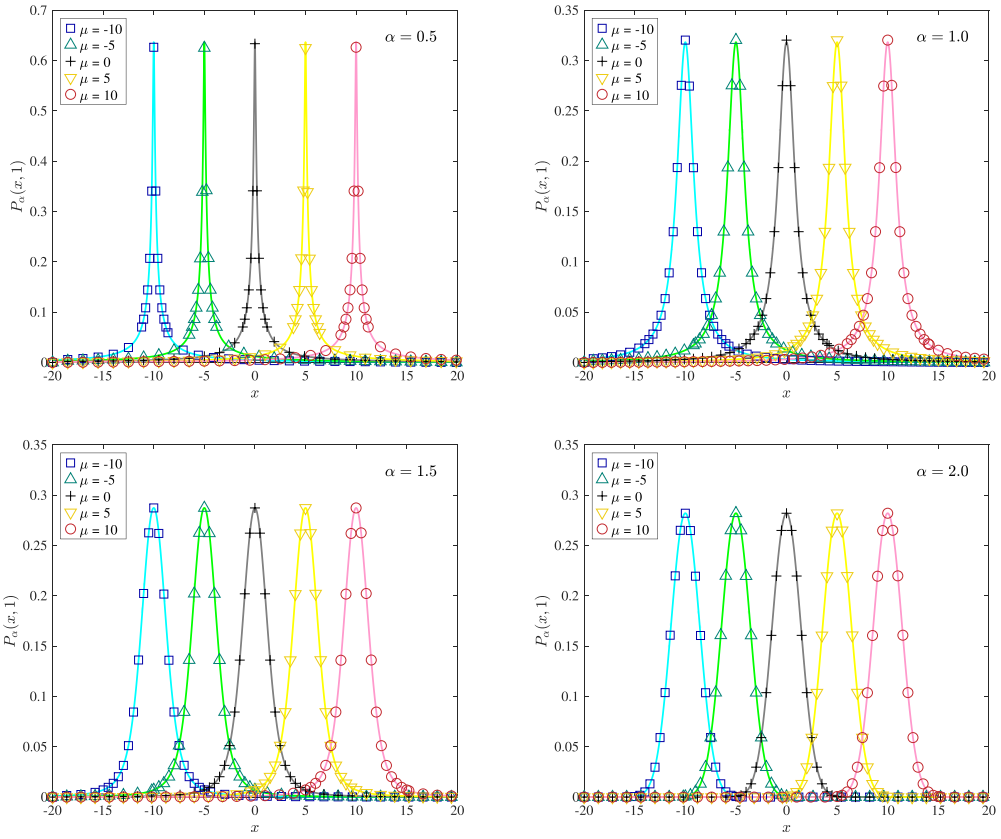

Figure 2. PDF of a symmetric α-stable probability law with drift for various parameters μ, is examined at $t=1$ within a domain of half-length $L=20$ and the initial condition $P_\alpha(x,0)=\delta(x)$. In all panels, symbols represent the numerical solution of the diffusion equation (6), while the lines depict the α-stable distributions obtained through the Fourier inversion of the characteristic function (7). The excellent agreement between the numerical solutions and the theoretical densities is evident. For all simulations, the time step is $\Delta t=0.001$ and the spatial step length is $\Delta x=0.01$.

the entire plotted range, the agreement between the numerical solutions and the theoretical densities is excellent.

3.3. Langevin equation

Conversely, the dynamic equation of Lévy flights in the presence of a constant drift is a stochastic differential equation, known as the overdamped Langevin equation for the coordinate $x(t)$ [92, 93],

$$\frac{\mathrm{d}}{\mathrm{d}t}x(t)=\mu+K_\alpha^{1/\alpha}\zeta(t)\,, \tag{8}$$

driven by white Lévy stable noise $\zeta(t)$ characterised by the same α and μ parameters as the space-fractional Fokker–Planck operator (6) and with unit scale parameter. We note that the drift parameter can be written as $\mu^{-1}=\gamma m$, in which m is the mass of the particle and γ denotes the friction coefficient characterising the dissipative interaction with the bath of surrounding

particles. The survival probability $S(t)$ and the first-passage time PDF can be constructed by the discretised version of the Langevin equation,

$$x(t+\Delta t) = x(t) + \mu\Delta t + K_\alpha^{1/\alpha}(\Delta t)^{1/\alpha}\zeta_t. \tag{9}$$

To construct an ensemble of N trajectories $x(t)$ with the initial condition $x(0)=0$ and the boundary at $x=d$, equation (9) is integrated up to the time τ when a particle crosses the absorbing boundaries for the first time, i.e. as long as $x(t)<d$. The PDF of first-passage times was estimated from the ensemble of N first-passage times τ and the survival probability was obtained as the complementary cumulative distribution of first-passage times. In the simulation, we used $N=10^5$ trajectories constructed with the Euler–Maruyama method (see equation (9)), with the integration time-step $\Delta t = 10^{-3}$. Random numbers distributed according to α-stable densities were generated by standard methods [94–96]. It is important to note that the numerical simulations based on the diffusion equation for $0<\alpha<1$ are highly computationally intensive. Therefore, we present only the results obtained from the Langevin equation for this case. For $\alpha=1$, we employ both approaches: the diffusion equation at short times and the Langevin equation at longer times. In contrast, for $1<\alpha<2$, we utilise both the Langevin equation and the diffusion equation to provide a comprehensive analysis.

4. Brownian motion with arbitrary drift

4.1. First-passage time

For Brownian motion, the PDF in unbounded space reads

$$P_2(x,t) = \frac{1}{\sqrt{4\pi K_2 t}}\exp\left(-\frac{(x-\mu t)^2}{4K_2 t}\right), \tag{10}$$

and applying the Skorokhod theorem (detailed in appendix B) leads to the first-passage time PDF

$$\wp(t) = \frac{d}{\sqrt{4\pi K_2 t^3}}\exp\left(-\frac{(d-\mu t)^2}{4K_2 t}\right), \tag{11}$$

which is the famous Lévy–Smirnov distribution representing a well-known result of the theory of Brownian motion with a drift [2]. We mention that by using the intuitive images method and the Green's function approach [2] (see equations (3.2.13) and (3.3.5) there) and the first-arrival theory [97] (see equation (E.7) there) a similar result (with a different sign for μ, due to a different setup) was obtained. In figure 3, top panels, we show the result of equation (11) and compare it with the numerical simulation of the space-fractional Fokker–Planck equation at short and long times. In the long-time limit we have

$$\wp(t) \sim \exp\left(-\frac{\mu^2 t}{4K_2}\right), \qquad t\to\infty. \tag{12}$$

As expected, and also can be seen from figure 3(top right), the PDF of the first-passage time decreases exponentially irrespective of the sign of the drift. Here and in the following, the symbol $\sim$ means asymptotic equality, $\simeq$ denotes asymptotic equality up to a prefactor, and $\approx$ means approximately equal. For positive values of the drift parameter, it is very likely that the particle will be absorbed very quickly, while for negative μ it is more likely that the particle will escape to $-\infty$. In both cases, the PDF of the first-passage time should become vanishingly small in the long time limit.

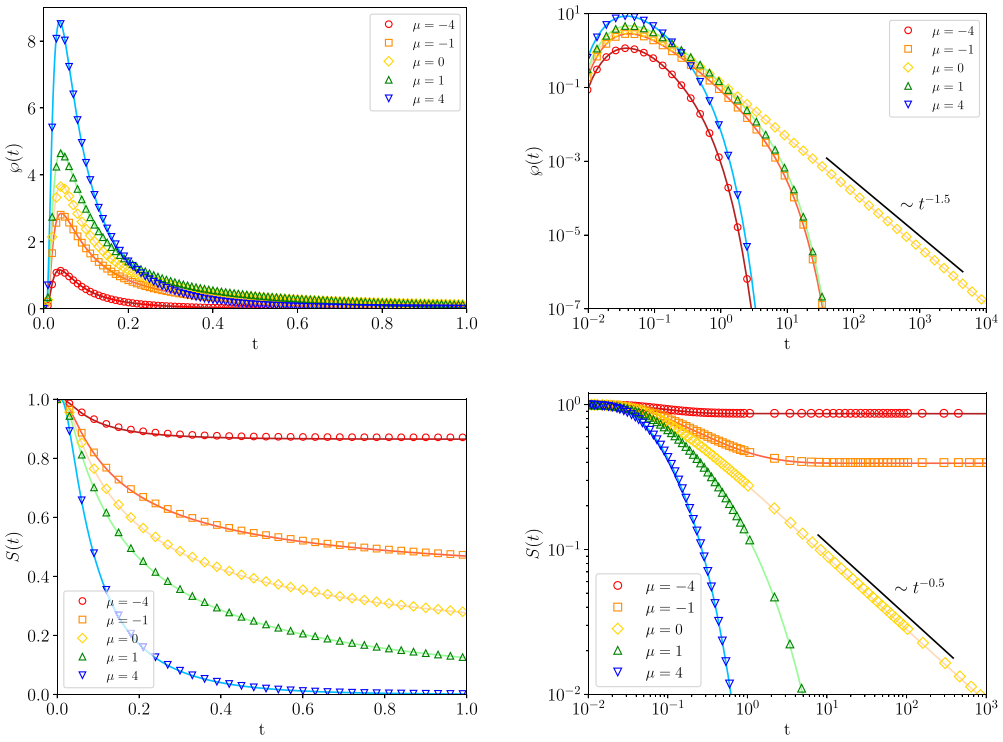

Figure 3. Top: first-passage time PDF for Brownian motion with a drift in a semi-infinite domain with $d = 0.5$ at short times on a linear scale (left) and at long times on a log–log scale (right). Symbols represent the numerical solution of the space-fractional diffusion equation (6) and the lines show the analytical result (11). The black short line on the right panel indicates a slope of $-3/2$ corresponding to the asymptotic behaviour of the first-passage time PDF for Brownian motion with $\mu = 0$. Bottom: survival probability of Brownian motion with a drift in a semi-infinite domain at short times on a linear scale (left) and at long times on a log–log scale (right). Symbols show the numerical solution of the space-fractional diffusion equation (6) and the lines are the analytical result (15). The black short line on the right panel indicates a slope of $-1/2$ corresponding to the asymptotic behaviour of the survival probability for Brownian motion with $\mu = 0$.

4.2. Survival probability

Integrating equation (1) the survival probability reads

$$S(t) = 1 - \int_0^t \wp\left(t'\right) \mathrm{d}t' . \tag{13}$$

By substitution of equation (11) into equation (13) we get

$$S(t) = 1 - \int_0^t \frac{d}{\sqrt{4\pi K_2 t'^3}} \exp\left(-\frac{\left(d - \mu t'\right)^2}{4K_2 t'}\right) \mathrm{d}t' . \tag{14}$$

Changing the variable according to $u^2 = d^2/4K_2t'$ leads us to

$$S(t) = 1 - \frac{2e^{\mu d/2K_2}}{\sqrt{\pi}} \int_{d/\sqrt{4K_2t}}^{\infty} \exp\left(-u^2 - (\mu d/4K_2u)^2\right) du$$
$$= \frac{1}{2}\left[\operatorname{erfc}\left(\frac{\mu t - d}{\sqrt{4K_2t}}\right) - e^{\frac{\mu d}{K_2}} \operatorname{erfc}\left(\frac{\mu t + d}{\sqrt{4K_2t}}\right)\right]. \tag{15}$$

From here we see that based on the sign of μ, the long-time asymptotic of the survival probability has the form

$$S(t) \sim \begin{cases} \sqrt{\frac{K_2}{\pi\mu^2 t}} e^{-\mu^2 t/4K_2}, & \mu > 0 \\ 1 - e^{-|\mu|d/K_2}, & \mu < 0 \end{cases}. \tag{16}$$

Thus, for a positive value of the drift parameter, the random walker is absorbed with certainty (*recurrent* process). For a negative value of μ, in contrast, the process is called *transient* and the random walker drifts toward $-\infty$ when t becomes large. A similar result using the image method in a different setup ($\mu \to -\mu$) was obtained in [2] (see equation (3.2.16)). In the case $\mu = 0$, we obtain $S(t) = \operatorname{erf}(d/\sqrt{4K_2t})$, which shows that the survival probability is almost constant until the diffusion length $\sqrt{K_2t}$ reaches the initial distance to the absorbing boundary d. When $\sqrt{K_2t} \gg d$, we have $S(t) \sim d/\sqrt{\pi K_2 t}$, showing the Sparre–Andersen law [98, 99]. In figure 3(bottom panels), we show the result for the survival probability by numerically solving the space-fractional diffusion equation (6) and compare it with the analytical result (15). As can be seen, when μ is positive, the survival probability decreases exponentially. Conversely, if it is negative ($\mu < 0$), the random walker moves preferentially in the negative direction, leading to the finite value $1 - \exp(-|\mu|d/K_2)$ for the survival probability (see equation (16)). We also note that the short-time limit of the survival probability is

$$S(t) \sim 1 - \sqrt{\frac{4K_2t}{\pi d^2}} \exp\left(-\frac{d^2}{4K_2t}\right), \quad t \to 0. \tag{17}$$

This result is independent of the drift parameter μ, indicating that the short-time behaviour is dominated solely by the diffusion coefficient K_2 and the length scale d.

5. Lévy flights with $\alpha = 1$ and arbitrary drift

For Lévy flights with the stability index, $\alpha = 1$ the distribution of jumps follows the Cauchy law

$$P_1(x,t) = \frac{1}{\pi} \frac{K_1 t}{(K_1 t)^2 + (x - \mu t)^2}. \tag{18}$$

In this section with the help of Skorokhod theorem we obtain the long time asymptotic behaviour of the first-passage time and the survival probability for Cauchy process with a drift.

5.1. First-passage time

In the presence of a constant drift μ, we obtain the long-time asymptotic of the first-passage time PDF as follows (see details in appendix C),

$$\wp(t) \sim \frac{1}{\pi}\left(\frac{d}{K_1}\right)^{\rho'} \left(\frac{t}{\sin(\pi\rho')}\right)^{-\rho'-1}, \tag{19}$$

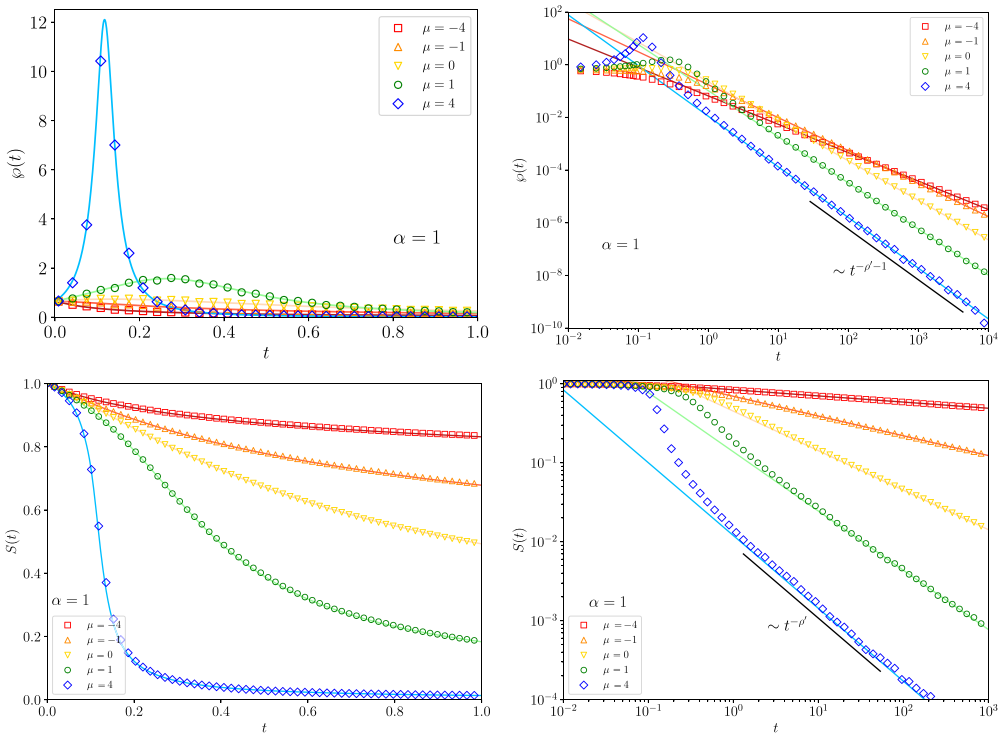

Figure 4. Top left: first-passage time PDF for the Cauchy process with a drift for different values of the drift parameter μ on a linear scale. Lines show the numerical results based on solving the space-fractional diffusion equation (6) and symbols are results obtained from the Langevin equation simulation. Top right: same as in the left panel on a log–log scale. Symbols represent the numerical solution of the Langevin equation, lines show equation (19) with the prefactor and the black short line shows the asymptote $t^{-\rho'-1}$. Bottom left: survival probability for the Cauchy process with a drift at different values of μ on linear scales. Numerical results are shown by lines based on the space-fractional diffusion equation (6), and symbols are from Langevin simulations. Bottom right: same as the left panel on a log–log scale. Symbols represent Langevin simulation results, and lines show equation (24) including the prefactor. The black short line indicates the asymptote $t^{-\rho'}$.

where this parameter ρ' is defined as

$$\rho' = \frac{1}{2} + \frac{1}{\pi}\arctan\left(\frac{\mu}{K_1}\right). \tag{20}$$

In figure 4 (top left panel), we show the short-time behaviour of the first-passage PDF for $\alpha = 1$ based on the numerical simulation of the space-fractional diffusion equation (6) and the Langevin equation (8). Moreover, on the top right panel of figure 4, we show the long-time asymptote of the first-passage PDF on a log–log scale based on the Langevin dynamics and compare it with equation (19). As can be seen, these two approaches agree perfectly in both panels and the prefactor shows good agreement with the theory. Note that in the case $\mu = 0$ we get the result in [43, 73],

$$\wp(t) \sim \frac{1}{\pi}\sqrt{\frac{d}{K_1}}t^{-3/2}. \tag{21}$$

In the limits $\mu \to \infty$ and $\mu \to -\infty$, by expansion of $\arctan(\mu/K_1)$ we have $\rho' \approx 1 - K_1/\pi\mu$ and $\rho' \approx K_1/\pi|\mu|$, respectively. Thus

$$\wp(t) \sim \begin{cases} \frac{dK_1}{\pi\mu^2} t^{-2}, & \mu \to \infty \\ \frac{K_1}{\pi|\mu|} t^{-1}, & \mu \to -\infty \end{cases}. \tag{22}$$

For $\mu \to \infty$, the first-passage time PDF decays as t^{-2}, with the prefactor scaling as μ^{-2}. This reflects the fact that, under a large positive drift, the particle is more likely to cross the absorbing boundary quickly, leading to a rapid decay of the PDF. In contrast, for $\mu \to -\infty$, the decay of the PDF follows t^{-1}, with a prefactor that scales as $|\mu|^{-1}$. In this case, the negative drift causes the particle to move away from the absorbing boundary, which increases the time it takes to cross. The slower decay indicates that the first-passage event occurs more gradually due to the opposing drift.

5.2. Survival probability

With the relation between the first-passage time and survival probability in the Laplace domain (see equations (2) and (C.16)) we find that

$$S(\lambda) \sim \frac{(d\sin(\pi\rho'))^{\rho'}}{K_1^{\rho'}\Gamma(1+\rho')} \lambda^{\rho'-1}. \tag{23}$$

Application of the inverse Laplace transform and using the reflection formula $\Gamma(z)\Gamma(1-z)\sin(\pi z) = \pi$, we find that

$$S(t) \sim \frac{1}{\pi\rho'} \left(\frac{d}{K_1}\right)^{\rho'} (\sin(\pi\rho'))^{\rho'+1} t^{-\rho'}. \tag{24}$$

In the bottom left panel of figure 4, we present the short-time behaviour of the survival probability for $\alpha = 1$, obtained from numerical simulations of the space-fractional diffusion equation (6) and the Langevin equation (8). The bottom right panel of figure 4 shows the long-time asymptote of the survival probability on a log–log scale, comparing Langevin simulation results with the theoretical expression from equation (24). As shown, the results from both approaches agree perfectly in both panels, and the prefactor aligns well with the theory. Again, using the expansion of $\arctan(\mu/K_1)$ in the limits $\mu \to \infty$ and $\mu \to -\infty$, corresponding to $\rho' \approx 1 - K_1/\pi\mu$ and $\rho' \approx K_1/\pi|\mu|$, respectively, we get the following results for the survival probability,

$$S(t) \sim \begin{cases} \frac{dK_1}{\pi\mu^2} t^{-1}, & \mu \to \infty \\ \exp\left(-\frac{K_1}{\pi|\mu|} \ln\left[\frac{K_1 t}{d}\right]\right), & \mu \to -\infty \end{cases}. \tag{25}$$

For $\mu \to \infty$, the survival probability decays as t^{-1}, with a prefactor scaling as μ^{-2}. This reflects the rapid crossing of the boundary d due to the strong positive drift, which accelerates the first-passage event. For $\mu \to -\infty$, the survival probability exhibits slower exponential decay with a logarithmic dependence on t. The negative drift opposes the motion, causing the particle to take longer to cross the threshold, resulting in a slower first-passage event.

6. Lévy flights with $0 < \alpha < 1$ and arbitrary drift

6.1. First-passage time

For this case, in the presence of small values of the drift parameter μ, we find the long-time asymptotic behaviour of the first-passage time PDF as follows (see appendix D for details),

$$\wp(t) \sim \frac{t^{-3/2}}{\Gamma(1+\alpha/2)} \sqrt{\frac{d^\alpha}{4\pi K_\alpha}} (1 - C_\alpha), \tag{26}$$

in which the constant C_α defined as

$$C_\alpha = \frac{\Gamma(1+\alpha/2)}{\Gamma(3\alpha/2)\cos(\pi\alpha/2)} \mathrm{Pe}_\alpha, \tag{27}$$

where Pe_α denotes the generalised Péclet number that quantifies the ratio between advective and diffusive transport rates with [40]

$$\mathrm{Pe}_\alpha = \frac{\mu d^{\alpha-1}}{2K_\alpha}. \tag{28}$$

In the limit where μ tends to zero, we refer to the findings in [43, 73]. The left panel of figure 5 illustrates the long-time behaviour of the first-passage time PDF governed by the α-stable distribution with stable index $\alpha = 0.5$, under the influence of μ. Conversely, the right panel of figure 5 showcases the long-time behaviour of the first-passage time PDF for symmetric α-stable distributions with various stable indices α and $\mu = -1$. Notably, as μ varies, the PDF demonstrates disparate decay rates: accelerated for $\mu > 0$ and decelerated for $\mu < 0$. Consequently, the role of μ primarily manifests in adjusting the prefactor, whereas the long time asymptotic behaviour of the first-passage time PDF remains consistent with the processes in absence of drift [43, 73]. The coefficient C_α corresponding to $\alpha = 0.5$ assumes values of $C_{0.5} = -0.74, 0, 0.74$ for $\mu = -1, 0,$ and 1, respectively. For $\mu = -1$, C_α varies as $C_\alpha = -0.43, -0.74, -1.8$ for $\alpha = 0.3, 0.5,$ and 0.8, respectively. It is important to note that equation (26) is derived under the assumption of a small drift parameter μ. Therefore, the prefactor is valid only in the regime where $|C_\alpha| < 1$. However, the long-time asymptote $\wp(t) \simeq t^{-3/2}$ is universal for $0 < \alpha < 1$ and holds for arbitrary μ (see figure 5).

6.2. Survival probability

Similarly, we find the long-time behaviour of the survival probability for small values of μ

$$S(t) \sim \frac{t^{-1/2}}{\Gamma(1+\alpha/2)} \sqrt{\frac{d^\alpha}{\pi K_\alpha}} (1 - C_\alpha), \tag{29}$$

where C_α is defined in equation (27). In the special case of $\mu = 0$, this result matches the one in [43, 73]. It is important to note that, due to the presence of long jumps when $0 < \alpha < 1$, the time exponent of the survival probability remains universal and does not depend on μ. The parameter μ only influences the prefactor $1 - C_\alpha$. As shown in the bottom left panel of figure 5(linear scale), the survival probability decays rapidly at short times for positive drift, reflecting particles crossing the boundary under the influence of the drift. However, the long-time asymptote universally decays as $t^{-1/2}$ in the log–log representation (bottom right panel), independent of μ. This behaviour highlights the dominance of long jumps in determining the escape dynamics when t becomes large.

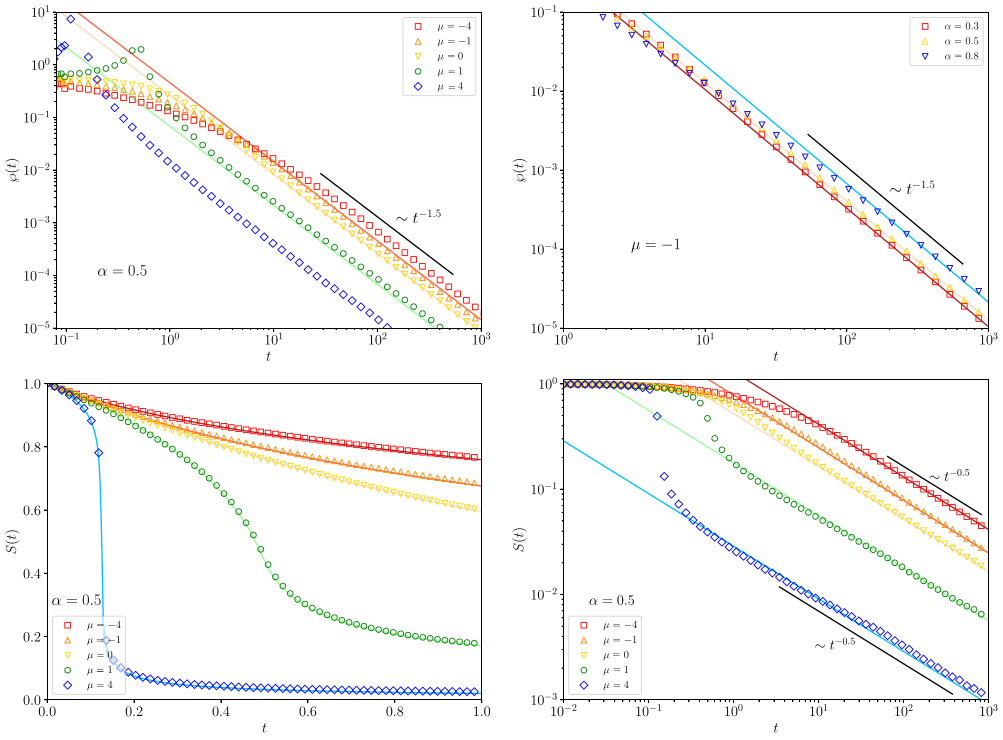

Figure 5. Top left: first-passage time PDF for a symmetric α-stable process with a drift and stable index $\alpha = 0.5$ in a semi-infinite domain with $d = 0.5$, shown in log–log scale for different values of μ. Top right: first-passage time PDF for different combinations of α and $\mu = -1$. In both panels, symbols are from Langevin equation simulations, lines represent equation (26), and the black short line indicates the long-time asymptote $t^{-3/2}$. Bottom: survival probability for the symmetric α-stable process with a drift and stable index $\alpha = 0.5$ for different μ. The left panel shows the results on a linear scale, and the right panel depicts the long-time behaviour on a log–log scale. Symbols represent Langevin equation simulations. In the left panel, lines show numerical results based on solving the space-fractional diffusion equation (6). In the right panel, lines represent equation (29) with the numerically obtained prefactor C_α, and the black short line indicates the long-time asymptote $t^{-1/2}$.

7. Lévy flights with $1 < \alpha < 2$ and negative drift

7.1. First-passage time

When the drift parameter is negative ($\mu < 0$), the random walker preferentially moves down the negative axis. We obtain the asymptote of the first-passage time PDF in the Laplace domain for $\mu < 0$ (detailed in appendix E), in the form

$$\wp(\lambda) \sim 1 - L_{\alpha-1,1}\left(\left(\frac{2|\mu|d^{\alpha-1}}{K_\alpha|\tan(\alpha\pi/2)|}\right)^{\frac{1}{\alpha-1}}, 1\right) - L_{\alpha-1,1}\left(\left(\frac{2|\mu|d^{\alpha-1}}{K_\alpha|\tan(\alpha\pi/2)|}\right)^{\frac{1}{\alpha-1}}, 1\right)\frac{K_\alpha/|\mu|^\alpha}{2|\cos(\alpha\pi/2)|}\lambda^{\alpha-1}, \quad \lambda \to 0, \tag{30}$$

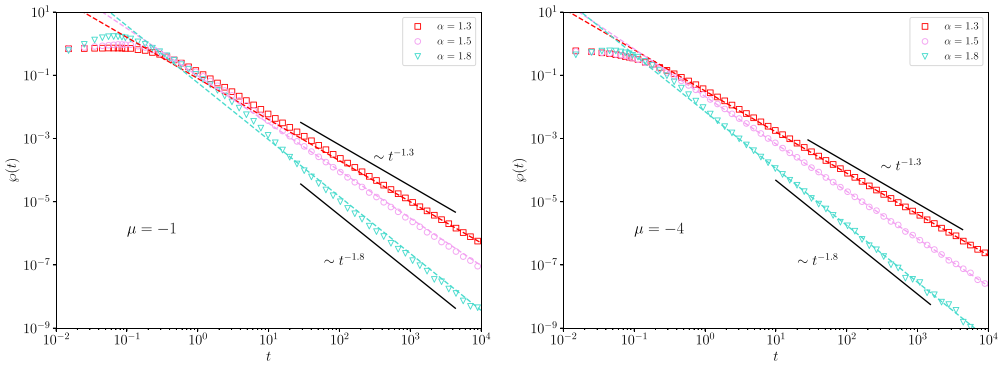

Figure 6. First-passage time PDF for symmetric α-stable probability law with $\mu = -1$ (left), and $\mu = -4$ (right) in a semi-infinite domain with $d = 0.5$ for different sets of the index of stability α obtained based on numerical results of the Langevin equation. The solid black lines show the asymptotic of the first-passage time PDF with $t^{-\alpha}$ (31), whereas the dashed lines show equation (31) with the prefactor.

where $L_{\alpha',\beta}(z)$ is the cumulative distribution of a one-sided α-stable probability law with $0 < \alpha' < 1$ and $\beta = 1$. Equation (30) is an improper PDF as $\wp(\lambda = 0) \neq 1$ [100, 101]. By applying the inverse Laplace transform, the long-time asymptotic of the first-passage time PDF reads

$$\wp(t) \sim \frac{K_\alpha \Gamma(\alpha) \sin(\alpha\pi/2)}{\pi |\mu|^\alpha} L_{\alpha-1,1}\left(\left(\frac{2|\mu| d^{\alpha-1}}{K_\alpha |\tan(\alpha\pi/2)|}\right)^{\frac{1}{\alpha-1}}, 1\right) t^{-\alpha}. \tag{31}$$

In figure 6 we plot the long-time asymptote of the first-passage time PDF on a log–log scale for different values of the stable index α, based on numerical simulation of the Langevin equation for $\mu = -1$ and -4. A comparison with equation (31) and its prefactor has been conducted, demonstrating excellent agreement with the numerical results. When comparing this with the case when $\mu = 0$, which corresponds to the well-known Sparre–Andersen law ($\wp(t) \simeq t^{-3/2}$) regardless of the stable index α, we conclude that for $1 < \alpha < 1.5$ the first-passage time PDF decays more slowly than in the scenario in absence of drift. Consequently, even though the walker typically drifts toward $-\infty$ when $\mu < 0$, rare large jumps contribute to increasingly higher values of the first-passage time PDF as t increases.

7.2. Survival probability

Using relation (2) between the first-passage time and survival probability in the Laplace domain, and referring to equation (30) for the case of a negative drift, we find that

$$S(\lambda) \sim L_{\alpha-1,1}\left(\left(\frac{2|\mu| d^{\alpha-1}}{K_\alpha |\tan(\alpha\pi/2)|}\right)^{\frac{1}{\alpha-1}}, 1\right) \frac{\exp\left(\frac{K_\alpha/|\mu|^\alpha}{2|\cos(\alpha\pi/2)|}\lambda^{\alpha-1}\right)}{\lambda}. \tag{32}$$

Applying the inverse Laplace transform leads us to

$$S(t) \sim L_{\alpha-1,1}\left(\left(\frac{2|\mu|d^{\alpha-1}}{K_\alpha|\tan(\alpha\pi/2)|}\right)^{\frac{1}{\alpha-1}},1\right) W_{1-\alpha,1}\left(\frac{K_\alpha/|\mu|^\alpha}{2|\cos(\alpha\pi/2)|}t^{1-\alpha}\right)$$
$$\sim L_{\alpha-1,1}\left(\left(\frac{2|\mu|d^{\alpha-1}}{K_\alpha|\tan(\alpha\pi/2)|}\right)^{\frac{1}{\alpha-1}},1\right), \tag{33}$$

where in the last equality we use the relation $W_{1-\alpha,1}(0)=1$ for the Wright function [102]. As seen in this scenario, the particles escape to $-\infty$, indicating that the negative drift is stronger than the diffusion term.

8. Lévy flights with $1<\alpha<2$ and positive drift

8.1. First-passage time

Finally in the case $\mu>0$, the random walker moves towards the boundary d. We find the following relation for the long-time asymptotic of the first-passage time PDF in the case $\mu>0$ (detailed in appendix E),

$$\wp(t) \sim \frac{K_\alpha f(\alpha,\mu,K_\alpha,d)}{2\mu^\alpha|\cos(\alpha\pi/2)|\Gamma(-\alpha)}t^{-\alpha-1}$$
$$\sim \frac{K_\alpha}{\pi\mu^\alpha}\sin\left(\frac{\alpha\pi}{2}\right)\Gamma(\alpha+1)f(\alpha,\mu,K_\alpha,d)\,t^{-\alpha-1}, \tag{34}$$

where $f(\alpha,\mu,K_\alpha,d)$ defined as (E.21) which can be computed numerically. In figure 7 we plot the first-passage time PDF of a symmetric α-stable process with positive μ on a log–log scale and compare the numerical results with equation (34). Moreover, in figure 8(top panels) we present the results for the first-passage time PDF of an α-stable process with $\alpha=1.5$ in a semi-infinite domain in the short-time (top left) and the long-time (top right) limits, based on the numerical simulation of the Langevin equation. In the short-time limit we compare the results with the numerical simulation of the space-fractional diffusion equation, and in the long-time limit we compare the Langevin simulation results with the analytical result in equations (31) and (34), all showing excellent agreement.

8.2. Survival probability

Based on relation (2) between the first-passage time and the survival probability in the Laplace domain we find that

$$S(\lambda) \sim f(\alpha,\mu,K_\alpha,d)\exp\left[-\frac{K_\alpha\lambda^{\alpha-1}}{2\mu^\alpha|\cos(\alpha\pi/2)|}\right], \tag{35}$$

where applying the inverse Laplace transform gives us

$$S(t) \sim f(\alpha,\mu,K_\alpha,d)\left(\frac{2\mu^\alpha}{K_\alpha|\tan(\alpha\pi/2)|}\right)^{\frac{1}{\alpha-1}} P_{\alpha-1,1}\left(\left(\frac{2\mu^\alpha t^{\alpha-1}}{K_\alpha|\tan(\alpha\pi/2)|}\right)^{\frac{1}{\alpha-1}},1\right). \tag{36}$$

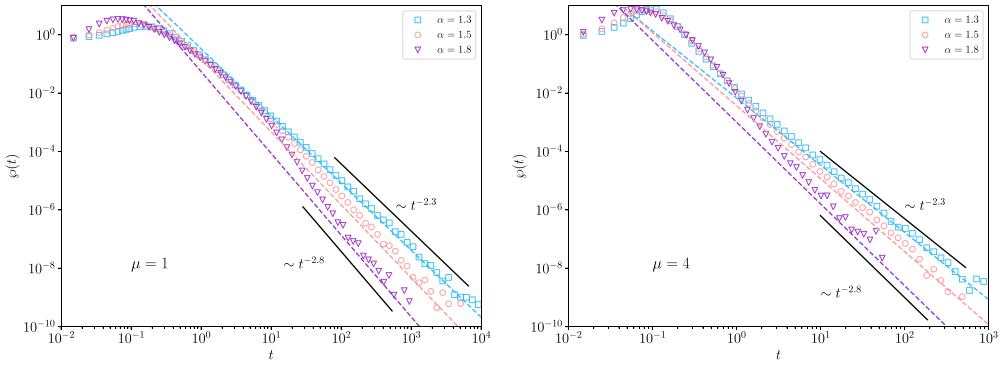

Figure 7. First-passage time PDF for symmetric α-stable probability law with $\mu = 1$ (left) and $\mu = 4$ (right) in a semi-infinite domain with $d = 0.5$ for different combinations of the index of stability α obtained from numerical results of the Langevin equation. The solid black lines show the asymptotic of the first-passage time PDF with $t^{-\alpha-1}$ (34). The dashed lines show equation (34) including the prefactor.

By simplification we get

$$S(t) \sim \frac{K_\alpha \sin(\alpha\pi/2)\,\Gamma(\alpha) f(\alpha,\mu,K_\alpha,d)}{\pi\mu^\alpha} t^{-\alpha}. \tag{37}$$

The survival probability for a symmetric α-stable process ($\alpha = 1.5$) on a semi-infinite domain is shown in the bottom panels of figure 8. The left panel compares numerical solutions of the space-fractional diffusion equation (lines) with Langevin equation simulations (symbols) on a linear scale, highlighting the μ-dependent short-time decay. The right panel reveals the asymptotic regimes on a log–log scale: for $\mu = 0$, the survival probability follows the Sparre–Andersen universality $S(t) \simeq t^{-1/2}$, while for $\mu > 0$, drift effects a steepening of the decay to $S(t) \simeq t^{-\alpha}$. For $\mu < 0$, the survival probability plateaus at long times due to drift-driven retention. This highlights how drift fundamentally alters escape dynamics, transitioning from the universal Sparre-Andersen scaling at $\mu = 0$ to drift-dominated dynamics when $\mu \neq 0$. In figure 9 we show the results for the survival probability of symmetric Lévy flights with a drift with stability index $\alpha = 1.3$ and $\alpha = 1.8$. As can be seen, in the absence of a drift for any symmetric jump length distribution in a Markovian setting the first-passage time PDF has the universal Sparre Andersen asymptotic $\wp(t) \simeq t^{-3/2}$ (and thus $S(t) \simeq t^{-1/2}$), whereas in the presence of a constant positive drift, it behaves as $\wp(t) \simeq t^{-1-\alpha}$(and thus $S(t) \simeq t^{-\alpha}$) for the stability index $1 < \alpha < 2$. We mention that in [75] by means of record statistics the asymptotic behaviour of the persistent probability (the probability that the stochastic process stays to the left of its initial starting position up to n steps) of a one-dimensional discrete-time random walk in the presence of a drift with symmetric jump distribution was studied (see equation (67) in [75]).

9. Discussion

First-passage time problems are crucial in understanding how stochastic processes behave when they first hit a boundary or exceed a threshold, providing insights into the dynamics of various physical and biological systems. These problems often involve analysing the first-passage time PDF to characterise the statistical properties and long-time behaviour of the

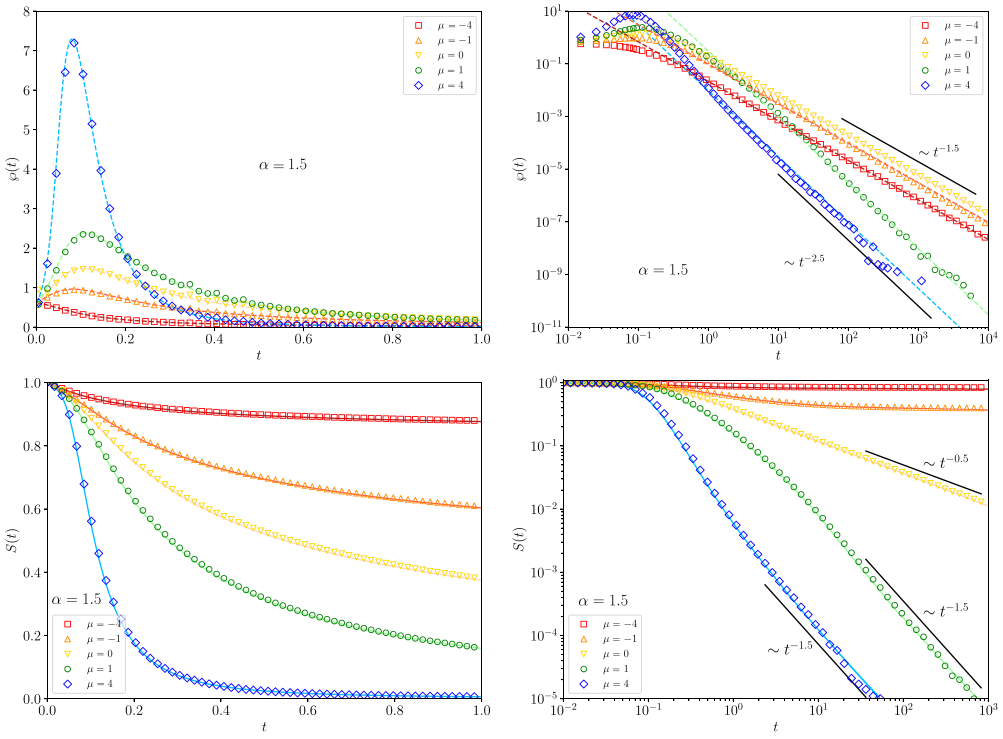

Figure 8. Top left: first-passage time PDF for symmetric α-stable probability law with $\alpha = 1.5$, in a semi-infinite domain with $d = 0.5$ for different values of the drift parameter μ in linear scale. Lines show numerical results based on solving the space-fractional diffusion equation (6), and symbols are obtained from Langevin equation simulations. Top right: the same as in the left panel on a log-log scale. Symbols represent the numerical solution of the Langevin equation (8), and dashed lines show the prefactor in equation (31) for $\mu < 0$ and equation (34) for $\mu > 0$. The black lines show the asymptotic of the first-passage time PDF with $t^{-\alpha}$ and $t^{-\alpha-1}$ for negative and positive μ, respectively. Bottom left: survival probability for symmetric α-stable density with $\alpha = 1.5$ on a semi-infinite domain with $d = 0.5$, for different values of the drift parameter μ, shown on a linear scale. Lines represent numerical results based on solving the space-fractional diffusion equation (6), and symbols correspond to Langevin equation simulations. Bottom right: same as the left panel on a log–log scale. Symbols represent Langevin equation solutions (8) and lines represent numerical results from solving the space-fractional diffusion equation (6). The black lines show the asymptotic behaviour of the survival probability with $t^{-1/2}$ for zero μ and $t^{-\alpha}$ for positive μ, while for negative μ, the survival probability tends to a finite value at long times.

underlying processes. In this study, we focused on the first-passage time PDF of Lévy flights with a drift within a one-dimensional semi-infinite domain, with specific attention to its behaviour in the long-time regime. The scenario entails a particle initiating its motion at the origin within this domain, with an absorbing boundary situated at a distance d to the right of the particle's starting position. The domain extends indefinitely to the left.

Our investigation begins with Brownian motion in the presence of a drift, where we used the Skorokhod theorem to derive exact analytical results for the first-passage time PDF. We compared these analytical results with numerical simulations based on the Brownian diffusion

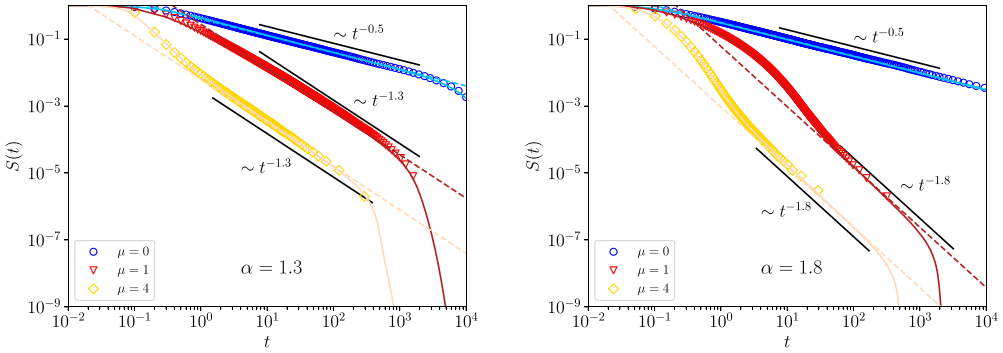

Figure 9. Survival probability for symmetric α-stable probability law in a semi-infinite domain with index $\alpha = 1.3$ (left) and $\alpha = 1.8$ (right) for different combinations of the drift parameter μ. The symbols represent simulation results based on the Langevin equation (8), while the lines correspond to numerical results based on the space-fractional diffusion equation (6). Dashed lines show equation (37) including the prefactor, and the black lines represent the universal Sparre Andersen scaling $S(t) \simeq t^{-1/2}$ for $\mu = 0$, and the asymptotic behaviour as $S(t) \simeq t^{-\alpha}$ for $\mu > 0$, which in the finite interval is eventually cut off by a steep exponential shoulder.

equation. This comparison confirmed the accuracy of our analytical expressions and highlighted the agreement between theory and numerical methods.

Next, we explored the case of a Cauchy processes ($\alpha = 1$) with a drift. We obtained the asymptotic behaviour of the first-passage time PDF and the survival probability for arbitrary drift values. Our analytical expressions were compared with numerical results obtained from the Langevin equation. The exponent of time t in these expressions was found to depend on the drift parameter, with the asymptotic behaviour varying accordingly.

For α-stable processes where $0 < \alpha < 1$, we derived the long-time asymptotic behaviour of the first-passage time PDF and survival probability for small drift values μ. Our findings revealed that as μ varies, the probability density demonstrates different decay rates: accelerated for $\mu > 0$ and decelerated for $\mu < 0$. Interestingly, the role of μ primarily affects the prefactor, while the long-time asymptotic behaviour remains consistent with the case without a drift [43, 73]. This observation was corroborated by our numerical simulations, which showed that the long-time asymptotic of the first-passage time PDF closely resembles that of the case without a drift, with only the prefactor affected by μ.

Finally, for α-stable processes with $1 < \alpha < 2$, our results showed distinct asymptotic behaviours depending on the direction and magnitude of the drift μ. Specifically, for negative drift ($\mu < 0$), the long-time behaviour follows a power-law decay of $t^{-\alpha}$, while for positive drift ($\mu > 0$), the decay is steeper, scaling as $t^{-\alpha-1}$. In the absence of a drift ($\mu = 0$), the decay reverts to the well-known $t^{-3/2}$ form, irrespective of α. Our study also revealed intriguing nuances in the tails of the first-passage time PDF, particularly for $1 < \alpha < 1.5$. For a negative drift ($\mu < 0$), the tails exhibited a less steep decay compared to the drift-free case, a phenomenon that can be explained by the PDF of jump lengths governed by α. As α increases, the likelihood of longer jumps decreases, affecting the boundary crossing probability over time.

In summary, our investigation underscores the intricate interplay between drift, stable index, and jump characteristics of Lévy flights. The results provide valuable insights into the long-time behaviour of first-passage time PDFs within semi-infinite domains, enriching our understanding of anomalous diffusion processes in complex systems. For a comprehensive overview

Table 1. First-passage time PDF for symmetric Lévy flights with different stable indices α in the presence of a constant drift μ.

α	μ	Exact PDF/Long-time asymptotic	Prefactor equation
2	Arbitrary	$\frac{d}{\sqrt{4\pi K_2 t^3}}\exp\left(-\frac{(d-\mu t)^2}{4K_2 t}\right)$ (11) [2, 97]	
1	Arbitrary	$\simeq t^{-3/2-\pi^{-1}\arctan(\mu/K_1)}$	(19), ($\mu=0$ [43, 73])
(0, 1)	Arbitrary	$\simeq t^{-3/2}$	(26), ($\mu=0$ [43, 73])
(1, 2)	$\mu<0$	$\simeq t^{-\alpha}$	(31)
	$\mu>0$	$\simeq t^{-\alpha-1}$	(34)
	$\mu=0$	$\simeq t^{-3/2}$ [67, 68]	[43, 73]

of the asymptotic behaviours across different stable indices and drift parameters, see table 1. Future investigations could explore the first-passage time statistics of asymmetric Lévy flights with a drift to determine how an asymmetry influences the short and long-time behaviours of the first-passage time PDF and the survival probability. This would enhance our understanding of how these processes behave within semi-infinite and finite domains. Finally, it would also be of interest to study the related distributions of extreme first-passage times [103, 104].

Data availability statement

No new data were created or analysed in this study.

Acknowledgment

A Ch and R M acknowledge support from the DFG projects 1535/12-1 and 1535/22-1. A Ch acknowledges support from the BMBF Project 01DK24006 PLASMA-SPIN-ENERGY. K C was supported by the Faculty of Physics, Astronomy and Applied Computer Science under the DSC 2019- N17/MNS/000013 scheme. This research was supported in part by PL-Grid Infrastructure. R M also acknowledges support from the Foundation for Polish Science (Fundacja na rzecz Nauki Polskiej) within an Alexander von Humboldt Polish Honorary Research Scholarship. Computer simulations were performed at the University of Potsdam, the Max-Planck Institute for the Physics of Complex Systems (Dresden, Germany) and the Academic Computer Center Cyfronet, AGH University of Science and Technology (Kraków, Poland) under CPU Grant 'DynStoch'.

Appendix A. A numerical scheme for fractional advection–diffusion equation

We here detail a specific implementation of the numerical approach based on the space-fractional Fokker–Planck equation in order to investigate the first-passage statistic of Lévy flights with a drift.

Among sparse numerical methods which are essentially different in the way of discretisation of normal and fractional derivatives, we mention, naming a few, the finite-difference scheme [105, 106], finite-element methods [107–109], and the spectral approach [110, 111]. Often it is more convenient to work with the finite-difference scheme to solve the space-fractional Fokker–Planck equation introduced in section 3. In this paper we implement the

modified trapezoidal rule algorithm [112, 113] to numerical integration of the fractional derivatives in Caputo form. For the first-order time derivative the first-order forward scheme has been used,

$$\frac{\partial}{\partial t}f(x_i,t_j)=\delta^1_- f_i^j\approx\frac{f_i^{j+1}-f_i^j}{\Delta t}, \tag{A.1}$$

where $f_i^j=f(x_i,t_j)$, $x_i=i\Delta x-L$ with step sizes in position $\Delta x=(d+L)/I$ and $i=0,1,2,\ldots,I$, $x_0=-L$, $x_I=d$. Similarly, $t_j=j\Delta t$ with time step $\Delta t=t/J$ and $j=0,1,2,\ldots,J-1$, $t_0=0$, $t_J=t$. Absorbing boundary conditions to investigate the first-passage statistics imply $f_0^j=f_I^j=0$ for all j. For the positive values of the drift parameter ($\mu=\mu_+$) and the left side space-fractional operator, the first-order space derivative of a function $f(x,t)$ is discretised by the second-order backward scheme, and similarly, for negative values of drift parameter ($\mu=\mu_-$) as well as the right side space-fractional operator, the first order space derivative of a function $f(x,t)$ is discretised by the second-order forward scheme, namely

$$\frac{\partial}{\partial x}f(x_i,t_j)=\delta^2_{\pm}f_i^j\approx\frac{\pm3f_i^j\mp4f_{i\mp1}^j\pm f_{i\mp2}^j}{2\Delta x}. \tag{A.2}$$

Moreover, for the second-order space-fractional derivatives we make use of the second-order central scheme according to

$$\frac{\partial^2}{\partial x^2}f(x_i,t_j)=\delta_c^2 f_i^j\approx\frac{-f_{i+2}^j+16f_{i+2}^j-30f_i^j+16f_{i-1}^j-f_{i-2}^j}{12\Delta x^2}. \tag{A.3}$$

For the right hand side of equation (6) first we write it in the Caputo form for the space-fractional derivatives, namely

$$\frac{\partial^\alpha}{\partial|x|^\alpha}f(x)=\begin{cases}-\frac{1}{2\cos(\pi\alpha/2)}\left({}_{-\infty}D_x^\alpha+{}_xD_\infty^\alpha\right)f(x), & \alpha\neq1\\ -\frac{\partial}{\partial x}\mathcal{H}\left\{f(x)\right\}, & \alpha=1\end{cases}, \tag{A.4}$$

where ${}_{-\infty}D_x^\alpha$ and ${}_xD_\infty^\alpha$ denote the left and right side space-fractional derivatives in the Caputo form, respectively $(n-1<\alpha<n)$ [114]

$${}_{-\infty}D_x^\alpha f(x)=\frac{1}{\Gamma(n-\alpha)}\int_{-\infty}^x\frac{f^{(n)}(u)}{(x-u)^{\alpha-n+1}}\mathrm{d}u, \tag{A.5}$$

$${}_xD_\infty^\alpha f(x)=\frac{(-1)^n}{\Gamma(n-\alpha)}\int_x^\infty\frac{f^{(n)}(u)}{(u-x)^{\alpha-n+1}}\mathrm{d}u. \tag{A.6}$$

Moreover, $\mathcal{H}$ in equation (A.4) denotes the Hilbert transform

$$\mathcal{H}\{f(x)\}=\frac{1}{\pi}\text{⨍}_{-\infty}^{\infty}\frac{f(u)}{x-u}\mathrm{d}u, \tag{A.7}$$

where the integral is to be taken as the principal value. By recalling the method introduced in [112] (theorem 3) we derive an algorithm to approximate the two-sided Caputo fractional derivatives of order $n-1<\alpha<n$. Concretely we apply the product trapezoidal quadrature formula [113], namely

$$\begin{aligned}&\int_{-L}^{x_i}\frac{f^{(n)}(\zeta,t_j)}{(x_i-\zeta)^{\alpha-n+1}}\mathrm{d}\zeta\\ &\quad\approx\sum_{k=1}^{i}\int_{x_{k-1}}^{x_k}\frac{1}{(x_i-\zeta)^{\alpha-n+1}}\left(\frac{x_k-\zeta}{x_k-x_{k-1}}f^{(n)}(x_{k-1},t_j)+\frac{\zeta-x_{k-1}}{x_k-x_{k-1}}f^{(n)}(x_k,t_j)\right)\mathrm{d}\zeta,\end{aligned} \tag{A.8}$$

for the left-side space-fractional operator, and

$$\int_{x_i}^{d} \frac{f^{(n)}(\zeta,t_j)}{(\zeta-x_i)^{\alpha-n+1}}\mathrm{d}\zeta \approx \sum_{k=i}^{I-1}\int_{x_k}^{x_{k+1}} \frac{1}{(\zeta-x_i)^{\alpha-n+1}}\left(\frac{x_{k+1}-\zeta}{x_{k+1}-x_k}f^{(n)}(x_k,t_j)+\frac{\zeta-x_k}{x_{k+1}-x_k}f^{(n)}(x_{k+1},t_j)\right)\mathrm{d}\zeta, \tag{A.9}$$

for the right-side space-fractional operator with the error estimate $\mathcal{O}(\Delta x^2)$ [115]. Using the relations

$$\int_a^b \frac{b-y}{[\pm(x-y)]^{1-\gamma}}\mathrm{d}y = \frac{1}{\gamma(\gamma+1)}\left([\pm(x-b)]^{\gamma+1}-([\pm(x-b)]-\gamma[\pm(b-a)])[\pm(x-a)]^{\gamma}\right), \tag{A.10}$$

and

$$\int_a^b \frac{y-a}{[\pm(x-y)]^{1-\gamma}}\mathrm{d}y = \frac{1}{\gamma(\gamma+1)}\left([\pm(x-a)]^{\gamma+1}-([\pm(x-a)]-\gamma[\pm(a-b)])[\pm(x-b)]^{\gamma}\right), \tag{A.11}$$

where the $+$ sign is taken for $x>b>a$ and the $-$ sign for $x<a<b$, equations (A.8) and (A.9) after simplification read

$$\int_{-L}^{x_i} \frac{f^{(n)}(\zeta,t_j)}{(x_i-\zeta)^{\alpha-n+1}}\mathrm{d}\zeta = \frac{\Delta x^{\gamma}}{\gamma(\gamma+1)}\sum_{k=0}^{i}\lambda_{k,i-k}f^{(n)}(x_k,t_j)+\mathcal{O}\left(\Delta x^2\right) \tag{A.12}$$

and

$$\int_{x_i}^{d} \frac{f^{(n)}(\zeta,t_j)}{(\zeta-x_i)^{\alpha-n+1}}\mathrm{d}\zeta = \frac{\Delta x^{\gamma}}{\gamma(\gamma+1)}\sum_{k=i}^{I}\lambda_{k,k-i}f^{(n)}(x_k,t_j)+\mathcal{O}\left(\Delta x^2\right) \tag{A.13}$$

respectively, in which $\gamma=n-\alpha$ and

$$\lambda_{k,m}=\begin{cases}(m-1)^{\gamma+1}-(m-\gamma-1)m^{\gamma}, & k=0,I\\ (m+1)^{\gamma+1}-2m^{\gamma+1}+(m-1)^{\gamma+1}, & 0<k<I,k\neq i\\ 1, & k=i\end{cases}. \tag{A.14}$$

For the special case $\alpha=1$, we approximate the derivative in space according to the method by [116], namely

$$\frac{\partial}{\partial x}\mathcal{H}\{f(x_i,t_j)\}=\frac{1}{\pi\Delta x}\left[\sum_{k=1}^{i}\lambda_{i-k}\left(f_k^j-f^j{}_{k-1}\right)+\sum_{k=i}^{I-1}\lambda_{k-i}\left(f_k^j-f^j{}_{k+1}\right)\right]+\mathcal{O}\left(\Delta x^2\right), \tag{A.15}$$

where $\lambda_m = 2/(2m+1)$. With the use of equations (A.4), (A.1) and (A.2) we can write Equation (6) on a discrete space-time grid as

$$\delta^1_{-} f_i^j + \mu_{\pm}\delta^2_{\pm} f_i^j = -\frac{K_\alpha}{2\cos(\pi\alpha/2)}\left[{}_{-L}D_x^\alpha f_i^j + {}_x D_d^\alpha f_i^j\right]. \tag{A.16}$$

By substitution of equations (A.1)–(A.3), (A.12) and (A.13) into equation (6) we obtain

$$\begin{aligned}\delta^1_{-} f_i^j + \mu_{\pm}\delta^2_{\pm} f_i^j = -\frac{K_\alpha \Delta x^{n-\alpha}}{2\cos(\pi\alpha/2)\Gamma(2+n-\alpha)}\Bigg[&\sum_{k=0}^{i}\lambda_{k,i-k}\delta^2_{+/c} f_k^j \\ &+(-1)^n\sum_{k=i}^{I}\lambda_{k,k-i}\delta^2_{-/c} f_k^j\Bigg].\end{aligned} \tag{A.17}$$

By defining

$$\begin{aligned}\Omega &= -\frac{K_\alpha \Delta t}{2\cos(\pi\alpha/2)\Gamma(2+n-\alpha)\Delta x^\alpha},\ 0<\alpha\leqslant 2, \alpha\neq 1\\ \Omega &= -\frac{K_\alpha \Delta t}{\pi\Delta x},\ \alpha = 1\\ \eta_{\pm} &= \frac{\mu_{\pm}\Delta t}{2\Delta x},\end{aligned} \tag{A.18}$$

for the case $n=1$ we obtain

$$\begin{aligned}f_i^{j+1} - f_i^j = -\eta_{\pm}\left(\pm 3f_i^j \mp 4f_{i\mp1}^j \pm f_{i\mp2}^j\right) + \frac{\Omega}{2}\Bigg[&\sum_{k=0}^{i}\lambda_{k,i-k}\left(3f_k^j - 4f_{k-1}^j + f_{k-2}^j\right)\\ &-\sum_{k=i}^{I}\lambda_{k,k-i}\left(-3f_k^j + 4f_{k+1}^j - f_{k+2}^j\right)\Bigg].\end{aligned} \tag{A.19}$$

After changing $f_i \to \theta f_i^{j+1} + (1-\theta)f_i^j$, $0\leqslant\theta\leqslant 1$, on the right hand side,

$$\begin{aligned}&f_i^{j+1} + \theta\Bigg[\eta_{\pm}(\pm 3f_i^{j+1} \mp 4f_{i\mp1}^{j+1} \pm f_{i\mp2}^{j+1}) - \frac{\Omega}{2}\Bigg(\sum_{k=0}^{i}\lambda_{k,i-k}(3f_k^{j+1} - 4f_{k-1}^{j+1} + f_{k-2}^{j+1})\\ &\quad+\sum_{k=i}^{I}\lambda_{k,k-i}(-3f_k^{j+1} + 4f_{k+1}^{j+1} - f_{k+2}^{j+1})\Bigg)\Bigg]\\ &= f_i^j - (1-\theta)\Bigg[\eta_{\pm}(\pm 3f_i^{j+1} \mp 4f_{i\mp1}^{j+1} \pm f_{i\mp2}^{j+1}) - \frac{\Omega}{2}\Bigg(\sum_{k=0}^{i}\lambda_{k,i-k}(3f_k^j - 4f_{k-1}^j + f_{k-2}^j)\\ &\quad+\sum_{k=i}^{I}\lambda_{k,k-i}(-3f_k^j + 4f_{k+1}^j - f_{k+2}^j)\Bigg)\Bigg].\end{aligned} \tag{A.20}$$

Following the similar procedure for the cases $1<\alpha<2$ and $\alpha=1$ we obtain

$$\left[\mathbf{I} + \theta\left(\eta_{\pm}\mathbf{V}^{\pm} + \Omega\mathbf{A}\right)\right]\mathbf{f}^{j+1} = \left[\mathbf{I} - (1-\theta)\left(\eta_{\pm}\mathbf{V}^{\pm} + \Omega\mathbf{A}\right)\right]\mathbf{f}^j, \tag{A.21}$$

in which the identity matrix $\mathbf{I}$ and the coefficient matrices $\mathbf{V}^{\pm}$ and $\mathbf{A}$ have dimension $(I+1)\times(I+1)$ and $j=0,1,2,\ldots,J-1$. The initial condition $f(x,0)=\delta(x)$ implemented by

$$f_i^0=\begin{cases}\frac{1}{\Delta x}, & i=L/\Delta x\\ 0, & \text{otherwise}\end{cases}. \tag{A.22}$$

Finally, the time evolution of the PDF is obtained by setting $f_0^j=f_I^j=0$ for all j as the absorbing boundary conditions.

The matrix $\mathbf{V}^{+}=-\mathbf{V}^{-T}$ has the form

$$\begin{aligned}&V^{+}_{m,m}=3, \quad 1\leqslant m\leqslant I+1\\ &V^{+}_{m+1,m}=-4, \quad 1\leqslant m\leqslant I\\ &V^{+}_{m+2,m}=1, \quad 1\leqslant m\leqslant I-1,\end{aligned} \tag{A.23}$$

and the matrix $\mathbf{A}$ can be written as $\mathbf{A}=\mathbf{R}+\mathbf{R}^{T}$, which for the three cases $0<\alpha<1$, $1<\alpha\leqslant 2$, and $\alpha=1$ is defined by

A.1 $0<\alpha<1$

$$\begin{aligned}&R_{m,m}=-\tfrac{3}{2}\lambda_{m,0}, \quad 1\leqslant m\leqslant I+1\\ &R_{m+1,m}=-\tfrac{3}{2}\lambda_{m,1}+2\lambda_{m+1,0}, \quad 1\leqslant m\leqslant I\\ &R_{m+n,m}=-\tfrac{3}{2}\lambda_{m,n}+2\lambda_{m+1,n-1}-\tfrac{1}{2}\lambda_{m+2,n-2}, \quad 2\leqslant n\leqslant I, \quad 1\leqslant m\leqslant I+1-n.\end{aligned} \tag{A.24}$$

A.2 $1<\alpha\leqslant 2$

$$\begin{aligned}&R_{m,m}=\tfrac{1}{12}\lambda_{m-1,2}-\tfrac{4}{3}\lambda_{m,1}+\tfrac{5}{2}\lambda_{m+1,0}, \quad 1\leqslant m\leqslant I+1\\ &R_{m,m+1}=\tfrac{1}{12}\lambda_{m,1}-\tfrac{4}{3}\lambda_{m+1,0}, \quad 1\leqslant m\leqslant I\\ &R_{m,m+2}=\tfrac{1}{12}\lambda_{m+1,0}, \quad 1\leqslant m\leqslant I-1\\ &R_{m+1,m}=\tfrac{1}{12}\lambda_{m-1,3}-\tfrac{4}{3}\lambda_{m,2}+\tfrac{5}{2}\lambda_{m+1,1}-\tfrac{4}{3}\lambda_{m+2,0}, \quad 1\leqslant m\leqslant I\\ &R_{m+n,m}=\tfrac{1}{12}\lambda_{m-1,n+2}-\tfrac{4}{3}\lambda_{m,n+1}+\tfrac{5}{2}\lambda_{m+1,n}-\tfrac{4}{3}\lambda_{m+2,n-1}+\tfrac{1}{12}\lambda_{m+3,n-2},\\ &\quad 2\leqslant n\leqslant I, \quad 1\leqslant m\leqslant I+1-n\end{aligned} \tag{A.25}$$

A.3 $\alpha=1$, $\beta=0$

$$\begin{aligned}&R_{m,m}=\lambda_0, \quad 1\leqslant m\leqslant I+1\\ &R_{m+n,m}=\lambda_n-\lambda_{n-1}, \quad 1\leqslant n\leqslant I, \quad 1\leqslant m\leqslant I+1-n.\end{aligned} \tag{A.26}$$

Appendix B. First-passage time PDF for Brownian motion with a drift

By substitution equation (10) into (5) we get

$$\frac{\partial}{\partial\lambda}\ln q_{+}(\lambda,k)=\int_0^{\infty}\mathrm{e}^{-\lambda t}\int_0^{\infty}\left(1-\mathrm{e}^{\mathrm{i}kx}\right)\frac{\mathrm{e}^{-(x-\mu t)^2/(4K_2t)}}{\sqrt{4\pi K_2 t}}\mathrm{d}x\,\mathrm{d}t. \tag{B.1}$$

Taking the integral over x produces

$$\begin{aligned}\frac{\partial}{\partial\lambda}\ln q_{+}(\lambda,k)&=\frac{1}{2}\int_0^{\infty}\mathrm{e}^{-\lambda t}\mathrm{erfc}\left(-\mu\sqrt{\frac{t}{4K_2}}\right)\mathrm{d}t\\ &\quad-\frac{1}{2}\int_0^{\infty}\mathrm{e}^{-\lambda t-k^2K_2t+\mathrm{i}k\mu t}\mathrm{erfc}\left(-\mathrm{i}k\sqrt{K_2t}-\mu\sqrt{\frac{t}{4K_2}}\right)\mathrm{d}t\\ &=\frac{1}{2}\left[\frac{\mu+\sqrt{4K_2\lambda+\mu^2}}{\lambda\sqrt{4K_2\lambda+\mu^2}}-\frac{2K_2\mathrm{i}k+\mu+\sqrt{4K_2\lambda+\mu^2}}{\left(K_2k^2-\mathrm{i}k\mu+\lambda\right)\sqrt{4K_2\lambda+\mu^2}}\right].\end{aligned} \tag{B.2}$$

By taking the indefinite integral over λ we obtain

$$q_+(\lambda,k)=\frac{\sqrt{4K_2\lambda+\mu^2}-\mu}{\sqrt{4K_2\lambda+\mu^2}-\mu-2K_2\mathrm{i}k}=\frac{\Lambda}{\Lambda-\mathrm{i}k}, \tag{B.3}$$

where $\Lambda=(\sqrt{4K_2\lambda+\mu^2}-\mu)/2K_2$. After an inverse Fourier transform according to equation (4) we arrive at ($x>0$)

$$\frac{\mathrm{d}}{\mathrm{d}x}p_+(\lambda,x)=\frac{1}{2\pi}\int_{-\infty}^{\infty}\mathrm{e}^{-\mathrm{i}kx}q_+(\lambda,k)\,\mathrm{d}k=\Lambda\exp(-\Lambda x). \tag{B.4}$$

Using the boundary condition ($p_+(\lambda,x)=0$ at $x\leqslant 0$) we get

$$p_+(\lambda,x)=\Lambda\int_0^x\exp(-\Lambda x)\,\mathrm{d}x=1-\exp(-\Lambda x), \tag{B.5}$$

and thus with the help of equation (3),

$$\wp(\lambda)=\exp(-\Lambda d)=\exp\left(-\frac{1}{2K_2}\left(\sqrt{\mu^2+4K_2\lambda}-\mu\right)d\right). \tag{B.6}$$

Finally, by making an inverse Laplace transform we get the desired result (11).

Appendix C. First-passage time PDF for the Cauchy process with a drift

Substitution of the PDF of the Cauchy process (18) into equation (5) yields

$$\frac{\partial}{\partial\lambda}\ln q_+(\lambda,k)=\int_0^\infty\mathrm{e}^{-\lambda t}\int_0^\infty\left(1-\mathrm{e}^{\mathrm{i}kx}\right)\frac{\pi^{-1}K_1t}{(K_1t)^2+(x-\mu t)^2}\mathrm{d}x\mathrm{d}t, \tag{C.1}$$

and after changing of the variable $y=(x-\mu t)/K_1t$, we obtain

$$\begin{aligned}\frac{\partial}{\partial\lambda}\ln q_+(\lambda,k)&=\int_0^\infty\mathrm{e}^{-\lambda t}\left[\frac{1}{\pi}\int_{-\mu/K_1}^\infty\frac{1}{1+y^2}\mathrm{d}y-\frac{\mathrm{e}^{\mathrm{i}k\mu t}}{\pi}\int_{-\mu/K_1}^\infty\frac{\mathrm{e}^{\mathrm{i}kK_1ty}}{1+y^2}\mathrm{d}y\right]\mathrm{d}t\\&=\frac{1}{\pi}\int_{-\mu/K_1}^\infty\frac{1}{1+y^2}\int_0^\infty\left[\mathrm{e}^{-\lambda t}-\mathrm{e}^{-(\lambda-\mathrm{i}k\mu-\mathrm{i}kK_1y)t}\right]\mathrm{d}t\mathrm{d}y.\end{aligned} \tag{C.2}$$

Then taking the integral over t, gives

$$\frac{\partial}{\partial\lambda}\ln q_+(\lambda,k)=\frac{1}{\pi}\int_{-\mu/K_1}^\infty\frac{1}{1+y^2}\left[\frac{1}{\lambda}-\frac{1}{\lambda-\mathrm{i}k\mu-\mathrm{i}kK_1y}\right]\mathrm{d}y. \tag{C.3}$$

From here taking the indefinite integral over λ leads to

$$\begin{aligned}\ln q_+(\lambda,k)&=\frac{1}{\pi}\int_{-\mu/K_1}^\infty\frac{1}{1+y^2}\ln\left(\frac{\lambda}{\lambda-\mathrm{i}k\mu-\mathrm{i}kK_1y}\right)\mathrm{d}y\\&=\frac{1}{\pi}\int_0^\infty\frac{1}{1+(u-\mu/K_1)^2}\ln\left(\frac{\lambda}{\lambda-\mathrm{i}kK_1u}\right)\mathrm{d}u,\end{aligned} \tag{C.4}$$

where in the last equality we use $u = y + \mu/K_1$. By taking the limit $\lambda \to 0$ we arrive at

$$\ln q_+(\lambda,k) \approx \frac{1}{\pi}\int_0^\infty \frac{\ln(\lambda/-\mathrm{i}kK_1)}{1+(u-\mu/K_1)^2}\mathrm{d}u - \frac{1}{\pi}\int_0^\infty \frac{\ln u}{1+(u-\mu/K_1)^2}\mathrm{d}u. \quad \text{(C.5)}$$

Then using the integrals

$$\int_0^\infty \frac{1}{(x+a)(x+b)}\mathrm{d}x = \frac{\ln a - \ln b}{a-b}, \quad \text{(C.6)}$$

$$\int_0^\infty \frac{\ln x}{(x+a)(x+b)}\mathrm{d}x = \frac{(\ln a)^2 - (\ln b)^2}{2(a-b)}, \quad \text{(C.7)}$$

and the relations

$$\operatorname{arccot}(x) = \frac{\mathrm{i}}{2}\ln\left(\frac{x-\mathrm{i}}{x+\mathrm{i}}\right), \quad \operatorname{arccot}(x) + \arctan(x) = \frac{\pi}{2}, \quad \text{(C.8)}$$

we obtain

$$\ln q_+(\lambda,k) \approx \left(\frac{1}{2} + \frac{1}{\pi}\arctan\left(\frac{\mu}{K_1}\right)\right)\ln\left(\frac{\lambda}{-\mathrm{i}kK_1}\right) - \frac{1}{4\pi\mathrm{i}}\left[\ln^2\left(\mathrm{i}-\frac{\mu}{K_1}\right) - \ln^2\left(-\mathrm{i}-\frac{\mu}{K_1}\right)\right]. \quad \text{(C.9)}$$

Thus

$$q_+(\lambda,k) \approx \left(\frac{\lambda}{-\mathrm{i}kK_1}\right)^{\frac{1}{2}+\frac{1}{\pi}\arctan\left(\frac{\mu}{K_1}\right)} \times \exp\left(-\frac{1}{4\pi\mathrm{i}}\left[\ln^2\left(\mathrm{i}-\frac{\mu}{K_1}\right) - \ln^2\left(-\mathrm{i}-\frac{\mu}{K_1}\right)\right]\right), \quad \lambda \to 0. \quad \text{(C.10)}$$

The argument of the exponential function can be simplified as follows,

$$\begin{aligned}&\ln^2\left(\mathrm{i}-\frac{\mu}{K_1}\right) - \ln^2\left(-\mathrm{i}-\frac{\mu}{K_1}\right)\\ &= \left[\ln\left(\mathrm{i}-\frac{\mu}{K_1}\right) - \ln\left(-\mathrm{i}-\frac{\mu}{K_1}\right)\right]\left[\ln\left(\mathrm{i}-\frac{\mu}{K_1}\right) + \ln\left(-\mathrm{i}-\frac{\mu}{K_1}\right)\right]\\ &= \ln\left(\frac{\frac{\mu}{K_1}-\mathrm{i}}{\frac{\mu}{K_1}+\mathrm{i}}\right)\ln\left(1+\frac{\mu^2}{K_1^2}\right) = 2\mathrm{i}\operatorname{arccot}\left(\frac{-\mu}{K_1}\right)\ln\left(1+\frac{\mu^2}{K_1^2}\right).\end{aligned} \quad \text{(C.11)}$$

Therefore equation (C.10) reads

$$q_+(\lambda,k) \approx \left(\frac{\lambda}{-\mathrm{i}kK_1}\right)^{\frac{1}{2}+\frac{1}{\pi}\arctan\left(\frac{\mu}{K_1}\right)}\left(1+\frac{\mu^2}{K_1^2}\right)^{-\frac{1}{2\pi}\operatorname{arccot}\left(\frac{-\mu}{K_1}\right)}, \quad \lambda \to 0. \quad \text{(C.12)}$$

Going back to equation (4) by inverse Fourier transform we find ($x > 0$)

$$\frac{\mathrm{d}}{\mathrm{d}x}p_+(\lambda,x) \approx \left(1+\frac{\mu^2}{K_1^2}\right)^{-\rho'/2} \frac{1}{2\pi}\int_{-\infty}^{\infty} \mathrm{e}^{-\mathrm{i}kx}\left(\frac{\lambda}{-\mathrm{i}kK_1}\right)^{\rho'} \mathrm{d}k$$
$$= \left(1+\frac{\mu^2}{K_1^2}\right)^{-\rho'/2} \left(\frac{\lambda}{K_1}\right)^{\rho'} \frac{x^{\rho'-1}}{\Gamma(\rho')}, \tag{C.13}$$

where

$$\rho' = \frac{1}{2} + \frac{1}{\pi}\arctan\left(\frac{\mu}{K_1}\right), \quad 0 \leqslant \rho' \leqslant 1. \tag{C.14}$$

With the boundary condition $p_+(\lambda, x=0)=0$ we arrive at

$$p_+(\lambda,x) \approx (\sin(\pi\rho'))^{\rho'} \left(\frac{\lambda}{K_1}\right)^{\rho'} \frac{x^{\rho'}}{\Gamma(1+\rho')}. \tag{C.15}$$

Following equation (3),

$$\wp(\lambda) \sim 1 - \frac{(d\sin(\pi\rho'))^{\rho'}}{K_1^{\rho'}\Gamma(1+\rho')}\lambda^{\rho'}, \tag{C.16}$$

and with the relation (2) between the first-passage time and survival probability in Laplace domain, we find

$$S(\lambda) \sim \frac{(d\sin(\pi\rho'))^{\rho'}}{K_1^{\rho'}\Gamma(1+\rho')}\lambda^{\rho'-1}. \tag{C.17}$$

Then, applying the inverse Laplace transform we get

$$S(t) \sim \frac{(d\sin(\pi\rho'))^{\rho'}}{K_1^{\rho'}\Gamma(1+\rho')\Gamma(1-\rho')}t^{-\rho'}. \tag{C.18}$$

From here by taking the first order time derivative (see equation (1)), we arrive at the corresponding result for the long-time asymptote of the first-passage time PDF (19) of Cauchy processes in the presence of a constant drift μ.

Appendix D. First-passage time PDF for α-stable processes with a drift and $0 < \alpha < 1$

We start from equation (4). With the help of the self-similar property

$$P_\alpha(x,t) = \frac{1}{(K_\alpha t)^{1/\alpha}} P_\alpha\left(\frac{x-\mu t}{(K_\alpha t)^{1/\alpha}}, 1\right), \tag{D.1}$$

and the change of variable $y = (x-\mu t)(K_\alpha t)^{-1/\alpha}$ we get

$$\ln q_+(\lambda,k) = \int_0^\infty \frac{\mathrm{e}^{-\lambda t}}{t}\int_{-\mu t(K_\alpha t)^{-1/\alpha}}^{\infty}\left[\mathrm{e}^{\mathrm{i}k(K_\alpha t)^{1/\alpha}y + \mathrm{i}k\mu t} - 1\right] P_\alpha(y,1)\,\mathrm{d}y\mathrm{d}t. \tag{D.2}$$

By splitting the inner integrals into two parts, we obtain

$$\ln q_+(\lambda,k) = A(\lambda,k) + B(\lambda,k), \tag{D.3}$$

where

$$A(\lambda,k)=\int_0^\infty \frac{\mathrm{e}^{-\lambda t}}{t}\int_0^\infty \left[\mathrm{e}^{\mathrm{i}k(K_\alpha t)^{1/\alpha}y+\mathrm{i}k\mu t}-1\right]P_\alpha(y,1)\,\mathrm{d}y\mathrm{d}t, \tag{D.4}$$

and

$$B(\lambda,k)=\int_0^\infty \frac{\mathrm{e}^{-\lambda t}}{t}\int_{-\mu t(K_\alpha t)^{-1/\alpha}}^0 \left[\mathrm{e}^{\mathrm{i}k(K_\alpha t)^{1/\alpha}y+\mathrm{i}k\mu t}-1\right]P_\alpha(y,1)\,\mathrm{d}y\mathrm{d}t. \tag{D.5}$$

Taking the λ-derivative of $A(\lambda,k)$ leads to

$$\begin{aligned}\frac{\partial}{\partial\lambda}A(\lambda,k)&=\int_0^\infty \mathrm{e}^{-\lambda t}\int_0^\infty \left[1-\mathrm{e}^{\mathrm{i}k(K_\alpha t)^{1/\alpha}y+\mathrm{i}k\mu t}\right]P_\alpha(y,1)\,\mathrm{d}y\mathrm{d}t\\&=\int_0^\infty \mathrm{e}^{-\lambda t}\int_0^\infty P_\alpha(y,1)\,\mathrm{d}y\mathrm{d}t\\&\quad-\int_0^\infty \mathrm{e}^{-\lambda t+\mathrm{i}k\mu t}\int_0^\infty \mathrm{e}^{\mathrm{i}k(K_\alpha t)^{1/\alpha}y}P_\alpha(y,1)\,\mathrm{d}y\mathrm{d}t.\end{aligned} \tag{D.6}$$

The first term on the right-hand side of equation (D.6) simply is $1/2\lambda$, and for the second term we employ theorem 2.6.2 from [90], which says that the one-sided Laplace transform with respect to y of an α-stable law $P_\alpha(y,1)$ has the form

$$P_\alpha(s,1)=\int_0^\infty \mathrm{e}^{-sy}P_\alpha(y,1)\,\mathrm{d}y=\frac{1}{\pi}\int_0^\infty \frac{\exp\left(-(sy)^\alpha\right)}{1+y^2}\mathrm{d}y. \tag{D.7}$$

Therefore, in the second term on the right-hand side of (D.6) we use equation (D.7) with $s\to-\mathrm{i}k(K_\alpha t)^{1/\alpha}$ and get

$$\begin{aligned}\frac{\partial}{\partial\lambda}A(\lambda,k)&=\frac{1}{2\lambda}-\frac{1}{\pi}\int_0^\infty \mathrm{e}^{-\lambda t+\mathrm{i}k\mu t}\int_0^\infty \frac{\exp\left(-(-\mathrm{i}ky)^\alpha K_\alpha t\right)}{1+y^2}\mathrm{d}y\mathrm{d}t\\&=\frac{1}{2\lambda}-\frac{1}{\pi}\int_0^\infty \frac{\left(\lambda-\mathrm{i}k\mu+K_\alpha(-\mathrm{i}ky)^\alpha\right)^{-1}}{1+y^2}\mathrm{d}y,\end{aligned} \tag{D.8}$$

where in the last equality we changed the order of integration and took the integrals over t. In the next step, we take the infinite integral over λ,

$$A(\lambda,k)=\frac{1}{2}\ln\lambda-\frac{1}{\pi}\int_0^\infty \frac{\ln\left[\lambda-\mathrm{i}k\mu+K_\alpha(-\mathrm{i}ky)^\alpha\right]}{1+y^2}\mathrm{d}y, \tag{D.9}$$

and then using

$$\begin{aligned}&\int_0^\infty \frac{\ln x}{a^2+x^2}\mathrm{d}x=\frac{\pi\ln a}{2a},\\&\int_0^\infty \frac{1}{a^2+x^2}\mathrm{d}x=\frac{\pi}{2a},\quad a>0,\end{aligned} \tag{D.10}$$

we get

$$A(\lambda,k)=\frac{1}{2}\ln\frac{\lambda}{K_\alpha(-\mathrm{i}k)^\alpha}-\frac{1}{\pi}\int_0^\infty \frac{\ln\left(1+\frac{\lambda-\mathrm{i}k\mu}{K_\alpha(-\mathrm{i}ky)^\alpha}\right)}{1+y^2}\mathrm{d}y. \tag{D.11}$$

In the limit $\lambda \to 0$ and for small values of μ, we can write

$$A(\lambda,k) \approx \frac{1}{2}\ln\frac{\lambda}{K_\alpha(-\mathrm{i}k)^\alpha} - \frac{1}{\pi}\int_0^\infty \frac{\ln\left(1+\frac{\mu}{K_\alpha}(-\mathrm{i}k)^{1-\alpha}y^{-\alpha}\right)}{1+y^2}\mathrm{d}y. \tag{D.12}$$

Using the relation

$$\ln(1+x) = -\sum_{n=1}^{\infty}\frac{(-x)^n}{n}, \quad |x| \leqslant 1, \ x \neq -1, \tag{D.13}$$

and taking the integral over y, we find

$$\begin{aligned} A(\lambda,k) &\approx \frac{1}{2}\ln\frac{\lambda}{K_\alpha(-\mathrm{i}k)^\alpha} + \frac{1}{2}\sum_{n=1}^{\infty}\frac{(-1)^n}{n\cos(n\pi\alpha/2)}\left(\frac{\mu}{K_\alpha}\right)^n(-\mathrm{i}k)^{n-n\alpha} \\ &\approx \frac{1}{2}\ln\frac{\lambda}{K_\alpha(-\mathrm{i}k)^\alpha} - \frac{\mu}{2K_\alpha\cos(\pi\alpha/2)}(-\mathrm{i}k)^{1-\alpha}. \end{aligned} \tag{D.14}$$

Now we go back to equation (D.5) and calculate $B(\lambda,k)$. Due to the symmetry of the PDF $P_\alpha(y,1) = P_\alpha(-y,1)$, we write $B(\lambda,k)$ as

$$\begin{aligned} B(\lambda,k) = &\int_0^\infty \frac{\mathrm{e}^{-\lambda t+\mathrm{i}k\mu t}}{t}\int_0^{\mu t(K_\alpha t)^{-1/\alpha}} \mathrm{e}^{-\mathrm{i}k(K_\alpha t)^{1/\alpha}y}P_\alpha(y,1)\,\mathrm{d}y\mathrm{d}t \\ &- \int_0^\infty \frac{\mathrm{e}^{-\lambda t}}{t}\int_0^{\mu t(K_\alpha t)^{-1/\alpha}} P_\alpha(y,1)\,\mathrm{d}y\mathrm{d}t. \end{aligned} \tag{D.15}$$

By looking at the upper limit of the inner integrals in equation (D.15) we notice that with $0<\alpha<1$, $\mu t(K_\alpha t)^{-1/\alpha} \to 0$ as $t \to \infty$. Therefore, we employ theorem 2.5.1 from [90] for the asymptotic representation of an α-stable law with $0<\alpha<1$, namely

$$P_\alpha(y,1) \sim \frac{1}{\pi}\Gamma(1+1/\alpha), \quad y \to 0. \tag{D.16}$$

Substitution of equation (D.16) into equation (D.15) and taking the integral first over y, we have

$$B(\lambda,k) \approx \frac{\Gamma(1+1/\alpha)}{-\mathrm{i}k\pi K_\alpha^{1/\alpha}}\int_0^\infty \frac{\mathrm{e}^{-\lambda t}}{t^{1+1/\alpha}}\left(1-\mathrm{e}^{\mathrm{i}k\mu t}+\mathrm{i}k\mu t\right)\mathrm{d}t. \tag{D.17}$$

When $\lambda \to 0$ we get

$$B(\lambda,k) \approx \frac{(\mu/K_\alpha)^{1/\alpha}}{\sin(\pi/\alpha)}(-\mathrm{i}k)^{-1+1/\alpha}. \tag{D.18}$$

Thus, $B(\lambda,k)$ is of the order of $\mu^{1/\alpha}$ and, in comparison with Equation (D.14), can be neglected. Therefore, substitution of equation (D.14) into equation (D.3) produces

$$\begin{aligned} q_+(\lambda,k) &\approx \sqrt{\frac{\lambda}{K_\alpha(-\mathrm{i}k)^\alpha}}\exp\left[-\frac{\mu}{2K_\alpha\cos(\pi\alpha/2)}(-\mathrm{i}k)^{1-\alpha}\right] \\ &\approx \sqrt{\frac{\lambda}{K_\alpha(-\mathrm{i}k)^\alpha}}\left(1-\frac{\mu}{2K_\alpha\cos(\pi\alpha/2)}(-\mathrm{i}k)^{1-\alpha}\right). \end{aligned} \tag{D.19}$$

By applying the inverse Fourier transform we find ($x>0$)

$$\begin{aligned}\frac{\mathrm{d}}{\mathrm{d}x}p_+(\lambda,x) &\approx \frac{1}{2\pi}\int_{-\infty}^{\infty}\mathrm{e}^{-\mathrm{i}kx}q_+(\lambda,k)\,\mathrm{d}k\\ &=\frac{1}{2\pi}\sqrt{\frac{\lambda}{K_\alpha}}\left(\int_{-\infty}^{\infty}\mathrm{e}^{-\mathrm{i}kx}(-\mathrm{i}k)^{-\alpha/2}\,\mathrm{d}k\right.\\ &\quad\left.-\frac{\mu}{2K_\alpha\cos(\pi\alpha/2)}\int_{-\infty}^{\infty}\mathrm{e}^{-\mathrm{i}kx}(-\mathrm{i}k)^{1-3\alpha/2}\,\mathrm{d}k\right)\\ &=\sqrt{\frac{\lambda}{K_\alpha}}\left(\frac{x^{-1+\alpha/2}}{\Gamma(\alpha/2)}-\frac{\mu}{2K_\alpha\cos(\pi\alpha/2)}\frac{x^{-2+3\alpha/2}}{\Gamma(-1+3\alpha/2)}\right),\end{aligned}\tag{D.20}$$

and with the boundary condition $p_+(\lambda,x=0)=0$,

$$p_+(\lambda,x)\approx\sqrt{\frac{\lambda}{K_\alpha}}\left(\frac{x^{\alpha/2}}{\Gamma(1+\alpha/2)}-\frac{\mu}{2K_\alpha\cos(\pi\alpha/2)}\frac{x^{-1+3\alpha/2}}{\Gamma(3\alpha/2)}\right).\tag{D.21}$$

Therefore with $\wp(\lambda)=1-p_+(\lambda,d)$,

$$\wp(\lambda)\sim 1-\sqrt{\frac{\lambda}{K_\alpha}}\left(\frac{d^{\alpha/2}}{\Gamma(1+\alpha/2)}-\frac{\mu}{2K_\alpha\cos(\pi\alpha/2)}\frac{d^{-1+3\alpha/2}}{\Gamma(3\alpha/2)}\right),\tag{D.22}$$

which due to $\wp(\lambda)=1-\lambda S(\lambda)$ results in

$$S(\lambda)\sim\sqrt{\frac{d^\alpha}{K_\alpha}}\left(\frac{1}{\Gamma(1+\alpha/2)}-\frac{\mu}{2K_\alpha\cos(\pi\alpha/2)}\frac{d^{-1+\alpha}}{\Gamma(3\alpha/2)}\right)\lambda^{-1/2}.\tag{D.23}$$

Then applying the inverse Laplace transform

$$S(t)\sim\sqrt{\frac{d^\alpha}{\pi K_\alpha}}\left(\frac{1}{\Gamma(1+\alpha/2)}-\frac{\mu}{2K_\alpha\cos(\pi\alpha/2)}\frac{d^{-1+\alpha}}{\Gamma(3\alpha/2)}\right)t^{-1/2}.\tag{D.24}$$

From here, the long-time asymptotic of the first-passage time PDF for the case $0<\alpha<1$ has the form

$$\wp(t)\sim\frac{t^{-3/2}}{\alpha\Gamma(\alpha/2)}\sqrt{\frac{d^\alpha}{\pi K_\alpha}}\left(1-\frac{\alpha\Gamma(\alpha/2)\,\mathrm{Pe}_\alpha}{2\cos(\pi\alpha/2)\Gamma(3\alpha/2)}\right).\tag{D.25}$$

Appendix E. First-passage time PDF for α-stable processes with a drift and $1<\alpha<2$

Similar to the last section, starting with equation (4) and using the self-similar property (D.1) along with the change of variable $y=(x-\mu t)(K_\alpha t)^{-1/\alpha}$, we get

$$\ln q_+(\lambda,k)=\int_0^\infty\frac{\mathrm{e}^{-\lambda t}}{t}\int_{\frac{-\mu t}{(K_\alpha t)^{1/\alpha}}}^{\infty}\left[\mathrm{e}^{\mathrm{i}k(K_\alpha t)^{1/\alpha}y+\mathrm{i}k\mu t}-1\right]P_\alpha(y,1)\,\mathrm{d}y\mathrm{d}t.\tag{E.1}$$

In the next step, we distinguish between the positive and negative drift parameters.

E.1. $\mu<0$

First, we consider the case $\mu<0$. It follows that when $t\to\infty$, the lower limit of the inner integral $|\mu|t\left(K_\alpha t\right)^{-1/\alpha}\to\infty$ for $1<\alpha<2$. Then it is reasonable to use the asymptotic expansion of an α-stable probability law $P_\alpha(y,1)$, namely,

$$P_\alpha\left(y,1\right)\sim\frac{1}{\pi}\Gamma\left(1+\alpha\right)\sin\left(\pi\alpha/2\right)y^{-\alpha-1},\quad y\to\infty. \tag{E.2}$$

Substitution of equation (E.2) into equation (E.1) yields

$$\ln q_+\left(\lambda,k\right)\approx\frac{1}{\pi}\Gamma\left(1+\alpha\right)\sin\left(\pi\alpha/2\right)\int_0^\infty\frac{\mathrm{e}^{-\lambda t}}{t}\int_{\frac{|\mu|t}{\left(K_\alpha t\right)^{1/\alpha}}}^\infty\left(\mathrm{e}^{\mathrm{i}k\left(K_\alpha t\right)^{1/\alpha}y-\mathrm{i}k|\mu|t}-1\right)\frac{\mathrm{d}y\mathrm{d}t}{y^{\alpha+1}}, \tag{E.3}$$

and changing the variable $u=yt^{-1+1/\alpha}$ produces

$$\ln q_+\left(\lambda,k\right)\approx\frac{1}{\pi}\Gamma\left(1+\alpha\right)\sin\left(\pi\alpha/2\right)\int_0^\infty\frac{\mathrm{e}^{-\lambda t}}{t^\alpha}\int_{\frac{|\mu|}{K_\alpha^{1/\alpha}}}^\infty\left(\mathrm{e}^{\mathrm{i}kK_\alpha^{1/\alpha}ut-\mathrm{i}k|\mu|t}-1\right)\frac{\mathrm{d}u\mathrm{d}t}{u^{\alpha+1.}} \tag{E.4}$$

Now we change the order of integral and first take the integral over t and then over u,

$$\begin{aligned}\ln q_+\left(\lambda,k\right)&\approx\frac{1}{\pi}\Gamma\left(1+\alpha\right)\sin\left(\pi\alpha/2\right)\int_{\frac{|\mu|}{K_\alpha^{1/\alpha}}}^\infty\frac{1}{u^{\alpha+1}}\int_0^\infty\left(\mathrm{e}^{-\lambda t+\mathrm{i}kK_\alpha^{1/\alpha}ut-\mathrm{i}k|\mu|t}-\mathrm{e}^{-\lambda t}\right)\frac{\mathrm{d}t\mathrm{d}u}{t^\alpha}\\&=\frac{1}{\pi}\Gamma\left(1+\alpha\right)\Gamma\left(1-\alpha\right)\sin\left(\pi\alpha/2\right)\int_{\frac{|\mu|}{K_\alpha^{1/\alpha}}}^\infty\frac{1}{u^{\alpha+1}}\left[\left(\lambda+\mathrm{i}k|\mu|-\mathrm{i}kK_\alpha^{1/\alpha}u\right)^{\alpha-1}-\lambda^{\alpha-1}\right]\mathrm{d}u\\&=-\frac{K_\alpha/|\mu|^\alpha}{2|\cos\left(\alpha\pi/2\right)|}\left(\frac{\lambda^\alpha-\left(-\mathrm{i}k|\mu|\right)^\alpha}{\lambda+\mathrm{i}k|\mu|}-\lambda^{\alpha-1}\right),\end{aligned} \tag{E.5}$$

where in the last equality we used the relation $\Gamma(1-z)\Gamma(z)\sin(\pi z)=\pi$. Therefore, in the limit of $\lambda\to0$, we get

$$q_+\left(\lambda,k\right)\approx\exp\left[-\frac{K_\alpha/|\mu|}{2|\cos\left(\alpha\pi/2\right)|}\left(\left(-\mathrm{i}k\right)^{\alpha-1}-\frac{\lambda^{\alpha-1}}{|\mu|^{\alpha-1}}\right)\right]. \tag{E.6}$$

Then the inverse Fourier transform of the above equation renders

$$\begin{aligned}\frac{\mathrm{d}}{\mathrm{d}x}p_+\left(\lambda,x\right)&=\frac{1}{2\pi}\int_{-\infty}^\infty\mathrm{e}^{-\mathrm{i}kx}q_+\left(\lambda,k\right)\mathrm{d}k\\&\approx\exp\left[\frac{K_\alpha/|\mu|^\alpha}{2|\cos\left(\alpha\pi/2\right)|}\lambda^{\alpha-1}\right]\frac{1}{2\pi}\int_{-\infty}^\infty\exp\left[-\mathrm{i}kx-\frac{K_\alpha|\tan\left(\alpha\pi/2\right)/\mu|}{2\cos\left(\left(\alpha-1\right)\pi/2\right)}\left(-\mathrm{i}k\right)^{\alpha-1}\right]\mathrm{d}k\\&\approx\exp\left[\frac{K_\alpha/|\mu|^\alpha}{2|\cos\left(\alpha\pi/2\right)|}\lambda^{\alpha-1}\right]\left(\frac{2|\mu|}{K_\alpha|\tan\left(\alpha\pi/2\right)|}\right)^{\frac{1}{\alpha-1}}P_{\alpha-1,1}\left(\left(\frac{2|\mu|x^{\alpha-1}}{K_\alpha|\tan\left(\alpha\pi/2\right)|}\right)^{\frac{1}{\alpha-1}},1\right),\end{aligned} \tag{E.7}$$

where $P_{\alpha,1}(z,1)$ is a one-sided α-stable probability law with the stable index $0<\alpha<1$. Applying the boundary condition $p_+(\lambda,x\leqslant0)=0$,

$$p_+\left(\lambda,x\right)\approx L_{\alpha-1,1}\left(\left(\frac{2|\mu|x^{\alpha-1}}{K_\alpha|\tan\left(\alpha\pi/2\right)|}\right)^{\frac{1}{\alpha-1}},1\right)\exp\left(\frac{K_\alpha/|\mu|^\alpha}{2|\cos\left(\alpha\pi/2\right)|}\lambda^{\alpha-1}\right), \tag{E.8}$$

where

$$L_{\alpha,1}(x,1) = \int_0^x P_{\alpha,1}(y,1)\,\mathrm{d}y$$
$$= 1 - \frac{1}{\pi}\sum_{n=1}^{\infty}(-1)^{n-1}\frac{\Gamma(n\alpha)}{\Gamma(1+n)}\sin(n\pi\alpha)\,x^{-n\alpha}, \quad \alpha < 1. \tag{E.9}$$

Thus, for the Laplace transform of the first-passage time PDF $\wp(\lambda) = 1 - p_+(\lambda, d)$ we have

$$\wp(\lambda) \sim 1 - L_{\alpha-1,1}\left(\left(\frac{2|\mu|d^{\alpha-1}}{K_\alpha|\tan(\alpha\pi/2)|}\right)^{\frac{1}{\alpha-1}}, 1\right)\exp\left(\frac{K_\alpha/|\mu|^\alpha}{2|\cos(\alpha\pi/2)|}\lambda^{\alpha-1}\right)$$
$$\sim 1 - L_{\alpha-1,1}\left(\left(\frac{2|\mu|d^{\alpha-1}}{K_\alpha|\tan(\alpha\pi/2)|}\right)^{\frac{1}{\alpha-1}}, 1\right)$$
$$- L_{\alpha-1,1}\left(\left(\frac{2|\mu|d^{\alpha-1}}{K_\alpha|\tan(\alpha\pi/2)|}\right)^{\frac{1}{\alpha-1}}, 1\right)\frac{K_\alpha/|\mu|^\alpha}{2|\cos(\alpha\pi/2)|}\lambda^{\alpha-1}, \quad \lambda \to 0. \tag{E.10}$$

By applying the inverse Laplace transform we finally arrive at the long-time asymptotic (31) of the first-passage time PDF for symmetric α-stable process with $1 < \alpha < 2$ and $\mu < 0$.

E.2. $\mu > 0$

In this case, it is convenient to use the relation

$$\int_{-a}^{\infty} f(y)\,\mathrm{d}y = \int_{-\infty}^{\infty} f(y)\,\mathrm{d}y - \int_{-\infty}^{-a} f(y)\,\mathrm{d}y = \int_{-\infty}^{\infty} f(y)\,\mathrm{d}y - \int_{a}^{\infty} f(-y)\,\mathrm{d}y, \tag{E.11}$$

to get from equation (4)

$$\ln q_+(\lambda,k) = \int_0^\infty \frac{\mathrm{e}^{-\lambda t}}{t}\left[\mathrm{e}^{\mathrm{i}k\mu t - tK_\alpha|k|^\alpha} - \mathrm{e}^{\mathrm{i}k\mu t}\int_{\frac{\mu t}{(K_\alpha t)^{1/\alpha}}}^{\infty}\mathrm{e}^{-\mathrm{i}k(K_\alpha t)^{1/\alpha}y}P_\alpha(y,1)\,\mathrm{d}y\right.$$
$$\left. + \int_{\frac{\mu t}{(K_\alpha t)^{1/\alpha}}}^{\infty} P_\alpha(y,1)\,\mathrm{d}y - 1\right]\mathrm{d}t. \tag{E.12}$$

Here we use the symmetric property $P_\alpha(y,1) = P_\alpha(-y,1)$ and the characteristic function of symmetric α-stable probability laws,

$$\int_{-\infty}^{\infty}\mathrm{e}^{\mathrm{i}ky(K_\alpha t)^{1/\alpha}}P_\alpha(y,1)\,\mathrm{d}y = \mathrm{e}^{-tK_\alpha|k|^\alpha}. \tag{E.13}$$

Next, by recalling equations (E.2) we write

$$\ln q_+(\lambda,k) \approx \int_0^\infty \frac{\mathrm{e}^{-\lambda t}}{t}\left[\mathrm{e}^{\mathrm{i}k\mu t - tK_\alpha|k|^\alpha} - 1\right]\mathrm{d}t - \frac{1}{\pi}\Gamma(1+\alpha)\sin(\alpha\pi/2)$$
$$\times \int_0^\infty \frac{\mathrm{e}^{-\lambda t}}{t}\left[\int_{\frac{\mu t}{(K_\alpha t)^{1/\alpha}}}^{\infty}\left(\mathrm{e}^{-\mathrm{i}k(K_\alpha t)^{1/\alpha}y + \mathrm{i}k\mu t} - 1\right)\frac{\mathrm{d}y}{y^{\alpha+1}}\right]\mathrm{d}t. \tag{E.14}$$

and changing the variable $u = yt^{-1+1/\alpha}$, to arrive at

$$\ln q_+(\lambda,k) \approx \int_0^\infty \frac{\mathrm{e}^{-\lambda t}}{t}\left[\mathrm{e}^{\mathrm{i}k\mu t - tK_\alpha|k|^\alpha} - 1\right]\mathrm{d}t - \frac{1}{\pi}\Gamma(1+\alpha)\sin(\alpha\pi/2) \times \int_0^\infty \frac{\mathrm{e}^{-\lambda t}}{t^\alpha}\left[\int_{\mu K_\alpha^{-1/\alpha}}^\infty \left(\mathrm{e}^{-\mathrm{i}kuK_\alpha^{1/\alpha}t + \mathrm{i}k\mu t} - 1\right)\frac{\mathrm{d}u}{u^{\alpha+1}}\right]\mathrm{d}t. \quad \text{(E.15)}$$

Changing the order of integration,

$$\begin{aligned}\ln q_+(\lambda,k) &\approx \int_0^\infty \frac{\mathrm{e}^{-\lambda t + \mathrm{i}k\mu t - K_\alpha|k|^\alpha t} - \mathrm{e}^{-\lambda t}}{t}\mathrm{d}t - \frac{1}{\pi}\Gamma(1+\alpha)\sin(\alpha\pi/2) \\ &\quad \times \int_{\mu K_\alpha^{-1/\alpha}}^\infty \frac{1}{u^{\alpha+1}}\int_0^\infty \frac{\mathrm{e}^{-\lambda t - \mathrm{i}kuK_\alpha^{1/\alpha}t + \mathrm{i}k\mu t} - \mathrm{e}^{-\lambda t}}{t^\alpha}\mathrm{d}t\mathrm{d}u \\ &= \ln\frac{\lambda}{\lambda - \mathrm{i}k\mu + K_\alpha|k|^\alpha} - \frac{1}{\pi}\Gamma(\alpha)\Gamma(1-\alpha)\sin(\alpha\pi/2) \\ &\quad \times \frac{K_\alpha}{\mu^\alpha}\left[\frac{\lambda^\alpha - (\mathrm{i}k\mu)^\alpha}{\lambda - \mathrm{i}k\mu} - \lambda^{\alpha-1}\right].\end{aligned} \quad \text{(E.16)}$$

Thus, in the limit $\lambda \to 0$ we get

$$q_+(\lambda,k) \approx \frac{\lambda}{-\mathrm{i}k\mu + K_\alpha|k|^\alpha}\exp\left(\frac{K_\alpha/\mu}{2|\cos(\alpha\pi/2)|}\left((\mathrm{i}k)^{\alpha-1} - \frac{\lambda^{\alpha-1}}{\mu^{\alpha-1}}\right)\right), \quad \lambda \to 0. \quad \text{(E.17)}$$

Therefore, $\mathrm{d}p_+(\lambda,x)/\mathrm{d}x$ follows by inverse Fourier transform of the above equation,

$$\begin{aligned}\frac{\mathrm{d}}{\mathrm{d}x}p_+(\lambda,x) &= \frac{1}{2\pi}\int_{-\infty}^\infty \mathrm{e}^{-\mathrm{i}kx}q_+(\lambda,k)\,\mathrm{d}k \\ &\approx \lambda\exp\left(-\frac{K_\alpha\lambda^{\alpha-1}}{2\mu^\alpha|\cos(\alpha\pi/2)|}\right)\frac{1}{2\pi}\int_{-\infty}^\infty \mathrm{e}^{-\mathrm{i}kx}\frac{\exp\left(\frac{K_\alpha(\mathrm{i}k)^{\alpha-1}}{2\mu|\cos(\alpha\pi/2)|}\right)}{-\mathrm{i}k\mu + K_\alpha|k|^\alpha}\mathrm{d}k,\end{aligned} \quad \text{(E.18)}$$

and with the boundary condition $p_+(\lambda, x \leqslant 0) = 0$ we get

$$p_+(\lambda,x) \approx \lambda\exp\left(-\frac{K_\alpha\lambda^{\alpha-1}}{2\mu^\alpha|\cos(\alpha\pi/2)|}\right)\frac{1}{2\pi}\int_{-\infty}^\infty \frac{1-\mathrm{e}^{-\mathrm{i}kx}}{\mathrm{i}k}\frac{\exp\left(\frac{K_\alpha(\mathrm{i}k)^{\alpha-1}}{2\mu|\cos(\alpha\pi/2)|}\right)}{-\mathrm{i}k\mu + K_\alpha|k|^\alpha}\mathrm{d}k. \quad \text{(E.19)}$$

Thus, for the Laplace transform of the first-passage time PDF $\wp(\lambda) = 1 - p_+(\lambda,d)$ we have

$$\begin{aligned}\wp(\lambda) &\sim 1 - \lambda\exp\left(-\frac{K_\alpha\lambda^{\alpha-1}}{2\mu^\alpha|\cos(\alpha\pi/2)|}\right)f(\alpha,\mu,K_\alpha,d) \\ &\sim 1 - f(\alpha,\mu,K_\alpha,d)\,\lambda + \frac{K_\alpha f(\alpha,\mu,K_\alpha,d)}{2\mu^\alpha|\cos(\alpha\pi/2)|}\lambda^\alpha, \ \ \lambda \to 0,\end{aligned} \quad \text{(E.20)}$$

where $f(\alpha,\mu,K_\alpha,d)$ is defined as

$$f(\alpha,\mu,K_\alpha,d) = \frac{1}{2\pi}\int_{-\infty}^\infty \frac{1-\mathrm{e}^{-\mathrm{i}kd}}{\mathrm{i}k}\frac{\exp\left(\frac{K_\alpha(\mathrm{i}k)^{\alpha-1}}{2\mu|\cos(\alpha\pi/2)|}\right)}{-\mathrm{i}k\mu + K_\alpha|k|^\alpha}\mathrm{d}k. \quad \text{(E.21)}$$

To make sure that $f(\alpha,\mu,K_\alpha,d)$ is a real-valued function, we consider the integrand

$$F(k)=\frac{1-\mathrm{e}^{-\mathrm{i}kd}}{\mathrm{i}k}\frac{\exp\left(\frac{K_\alpha(\mathrm{i}k)^{\alpha-1}}{2\mu|\cos(\alpha\pi/2)|}\right)}{-\mathrm{i}k\mu+K_\alpha|k|^{\alpha}.} \tag{E.22}$$

and check that the complex conjugate $\overline{F(-k)}=F(k)$. Thus the imaginary parts cancel and the function $f(\alpha,\mu,K_\alpha,d)$ is indeed a real-valued function,

$$f(\alpha,\mu,K_\alpha,d)=\frac{1}{\pi}\int_0^\infty \mathrm{Re}\left[F(k)\right]\mathrm{d}k. \tag{E.23}$$

Finally, by applying the inverse Laplace transform we arrive at the desired result (34).

ORCID iDs

Amin Padash https://orcid.org/0000-0002-3289-6556
Karol Capała https://orcid.org/0000-0002-8864-0760
Holger Kantz https://orcid.org/0000-0001-6921-6094
Bartłomiej Dybiec https://orcid.org/0000-0002-6540-3906
Babak Shokri https://orcid.org/0000-0002-8242-5111
Ralf Metzler https://orcid.org/0000-0002-6013-7020
Aleksei V Chechkin https://orcid.org/0000-0002-3803-1174

References

[1] Grebenkov D, Metzler R and Oshanin G 2025 *Target Search Problems* (Springer)
[2] Redner S 2001 *A Guide to First-Passage Processes* (Cambridge University Press)
[3] Metzler R, Redner S and Oshanin G 2014 *First-Passage Phenomena and Their Applications* (World Scientific)
[4] Bray A J, Majumdar S N and Schehr G 2013 Persistence and first-passage properties in nonequilibrium systems *Adv. Phys.* **62** 225
[5] Wang B, Kuo J, Bae S C and Granick S 2012 When Brownian diffusion is not Gaussian *Nat. Mater.* **11** 481
[6] Vaccario G, Antoine C and Talbot J 2015 First-passage times in d-dimensional heterogeneous media *Phys. Rev. Lett.* **115** 240601
[7] Newby J and Allard J 2016 First-passage time to clear the way for receptor-ligand binding in a crowded environment *Phys. Rev. Lett.* **116** 128101
[8] Lindsay A E, Bernoff A J and Ward M J 2017 First passage statistics for the capture of a Brownian particle by a structured spherical target with multiple surface traps *Multiscale Model. Simul.* **15** 74
[9] Bouchaud J-P and Potters M 2000 *Theory of Financial Risk and Derivative Pricing: From Statistical Physics to Risk Management* (Cambridge University Press)
[10] Zsurkis G, Nicolau J and Rodrigues P M 2024 First passage times in portfolio optimization: a novel nonparametric approach *Eur. J. Oper. Res.* **312** 1074
[11] Goeppert N, Goldscheider N and Berkowitz B 2020 Experimental and modeling evidence of kilometer-scale anomalous tracer transport in an alpine karst aquifer *Water Res.* **178** 115755
[12] Hufnagel L, Brockmann D and Geisel T 2004 Forecast and control of epidemics in a globalized world *Proc. Natl Acad. Sci. USA* **101** 15124
[13] Gross B, Zheng Z, Liu S, Chen X, Sela A, Li J, Li D and Havlin S 2020 Spatio-temporal propagation of COVID-19 pandemics *Europhys. Lett.* **131** 58003
[14] Metzler R, Barkai E and Klafter J 1999 Deriving fractional Fokker-Planck equations from a generalised master equation *Europhys. Lett.* **46** 431
[15] Wirner F, Scholz C and Bechinger C 2014 Geometrical interpretation of long-time tails of first-passage time distributions in porous media with stagnant parts *Phys. Rev.* E **90** 013025

[16] Wilemski G and Fixman M 1974 Diffusion-controlled intrachain reactions of polymers. I theory *J. Chem. Phys.* **60** 866
[17] Wilemski G and Fixman M 1974 Diffusion-controlled intrachain reactions of polymers. II results for a pair of terminal reactive groups *J. Chem. Phys.* **60** 878
[18] Szabo A, Schulten K and Schulten Z 1980 First passage time approach to diffusion controlled reactions *J. Chem. Phys.* **72** 4350
[19] Godec A and Metzler R 2016 Universal proximity effect in target search kinetics in the few-encounter limit *Phys. Rev.* X **6** 041037
[20] Grebenkov D S, Metzler R and Oshanin G 2018 Strong defocusing of molecular reaction times results from an interplay of geometry and reaction control *Commun. Chem.* **1** 96
[21] Hänggi P and Talkner P 1985 First-passage time problems for non-Markovian processes *Phys. Rev.* A **32** 1934
[22] Masoliver J, Lindenberg K and West B J 1986 First-passage times for non-Markovian processes: correlated impacts on bound processes *Phys. Rev.* A **34** 2351
[23] Sokolov I M 2003 Cyclization of a polymer: first-passage problem for a non-Markovian process *Phys. Rev. Lett.* **90** 080601
[24] Guérin T, Bénichou O and Voituriez R 2012 Non-Markovian polymer reaction kinetics *Nat. Chem.* **4** 568
[25] Likthman A E and Marques C M 2006 First-passage problem for the Rouse polymer chain: an exact solution *Europhys. Lett.* **75** 971
[26] Hedström L, Metzler R and Lizana L 2024 Enhancer-insulator pairing reveals heterogeneous dynamics in long-distance 3D gene regulation *PRX Life* **2** 033008
[27] Lomholt M A, Koren T, Metzler R and Klafter J 2008 Lévy strategies in intermittent search processes are advantageous *Proc. Natl Acad. Sci. USA* **105** 11055
[28] Condamin S, Bénichou O, Tejedor V, Voituriez R and Klafter J 2007 First-passage times in complex scale invariant media *Nature* **450** 77
[29] Condamin S, Tejedor V, Voituriez R, Bénichou O and Klafter J 2008 Probing microscopic origins of confined subdiffusion by first-passage observables *Proc. Natl Acad. Sci. USA* **105** 5675
[30] Godec A and Metzler R 2016 First passage time distribution in heterogeneity controlled kinetics: going beyond the mean first passage time *Sci. Rep.* **6** 20349
[31] Goychuk I and Hanggi P 2007 Anomalous escape governed by thermal $1/f$ noise *Phys. Rev. Lett.* **99** 200601
[32] Sliusarenko O Y, Gonchar V Y, Chechkin A V, Sokolov I M and Metzler R 2012 Kramers-like escape driven by fractional Gaussian noise *Phys. Rev.* E **81** 041119
[33] Capała K, Padash A, Chechkin A V, Shokri B, Metzler R and Dybiec B 2020 Lévy noise-driven escape from arctangent potential wells *Chaos* **30** 123103
[34] Lloyd A L and May R M 2001 How viruses spread among computers and people *Science* **292** 1316
[35] Ptaszynski K 2018 First-passage times in renewal and nonrenewal systems *Phys. Rev.* E **97** 012127
[36] Palyulin V V, Ala-Nissila T and Metzler R 2014 Polymer translocation: the first two decades and the recent diversification *Soft Matter* **10** 9016
[37] Dubbeldam J L A, Rostiashvili V G, Milchev A and Vilgis T A 2011 Fractional Brownian motion approach to polymer translocation: the governing equation of motion *Phys. Rev.* E **83** 0118028
[38] Palyulin V V, Blackburn G, Lomholt M A, Watkins N W, Metzler R, Klages R and Chechkin A V 2019 First passage and first hitting times of Lévy flights and Lévy walks *New J. Phys.* **21** 103028
[39] Padash A, Sandev T, Kantz H, Metzler R and Chechkin A V 2022 Asymmetric Lévy flights are more efficient in random search *Frac. Fract.* **6** 260
[40] Palyulin V V, Chechkin A V and Metzler R 2014 Lévy flights do not always optimize random blind search for sparse targets *Proc. Natl Acad. Sci. USA* **111** 2931
[41] Gomez D and Lawley S D 2024 First hitting time of a one-dimensional Lévy flight to small targets *SIAM J. Appl. Math.* **84** 1140
[42] Koren T, Chechkin A V and Klafter J 2007 On the first passage time and leapover properties of Lévy motions *Physica* A **379** 10
[43] Koren T, Lomholt M A, Chechkin A V, Klafter J and Metzler R 2007 Leapover lengths and first passage time statistics for Lévy flights *Phys. Rev. Lett.* **99** 160602
[44] Wardak A 2020 First passage leapovers of Lévy flights and the proper formulation of absorbing boundary conditions *J. Phys. A: Math. Theor.* **53** 375001
[45] Radice M and Cristadoro G 2024 Optimizing leapover lengths of Lévy flights with resetting *Phys. Rev.* E **110** L022103

[46] Mandelbrot B 1997 *The Fractal Geometry of Nature* (Freeman)
[47] Hughes B D 1995 *Random Walks and Random Environments (Vol 1: Randomwalks)* (Oxford University Press)
[48] Bouchaud J P and Georges A 1990 Anomalous diffusion in disordered media: statistical mechanisms, models and physical applications *Phys. Rep.* **195** 127
[49] Metzler R and Klafter J 2000 The random walk's guide to anomalous diffusion: a fractional dynamics approach *Phys. Rep.* **339** 1
[50] Metzler R and Klafter J 2004 The restaurant at the end of the random walk: recent developments in the description of anomalous transport by fractional dynamics *J. Phys A: Math. Gen.* **37** R161
[51] Lévy P 1954 *Théorie de l'addition des variables aléatoires* (Gauthier-Villars)
[52] Wang W and Barkai E 2020 Fractional advection-diffusion-asymmetry equation *Phys. Rev. Lett.* **125** 240606
[53] Wang W and Barkai E 2024 Fractional advection diffusion asymmetry equation, derivation, solution and application *J. Phys. A: Math. Theor.* **57** 035203
[54] Brockmann D, Hufnagel L and Geisel T 2006 The scaling laws of human travel *Nature* **439** 462
[55] González M C, Hidalgo C A and Barabási A-L 2008 Understanding individual human mobility patterns *Nature* **453** 779
[56] Bartumeus F, Da Luz M G E, Viswanathan G M and Catalan J 2005 Animal search strategies: a quantitative random-walk analysis *Ecology* **86** 3078
[57] Barthelemy P, Bertolotti J and Wiersma D A 2008 Lévy flight for light *Nature* **453** 495
[58] Caspi A, Granek R and Elbaum M 2000 Enhanced diffusion in active intracellular transport *Phys. Rev. Lett.* **85** 5655
[59] Gal N and Weihs D 2010 Experimental evidence of strong anomalous diffusion in living cells *Phys. Rev.* E **81** 020903
[60] Chen K J, Wang B and Granick S 2015 Memoryless self-reinforcing directionality in endosomal active transport within living cells *Nat. Mater.* **14** 589
[61] Song M S, Moon H C, Jeon J-H and Park H Y 2018 Neuronal messenger ribonucleoprotein transport follows an aging Lévy walk *Nat. Commun.* **9** 1
[62] del-Castillo-Negrete D and Chacón L L 2011 Local and nonlocal parallel heat transport in general magnetic fields *Phys. Rev. Lett.* **106** 195004
[63] Blazevski D and del-Castillo-Negrete D 2013 Local and nonlocal anisotropic transport in reversed shear magnetic fields: shearless cantori and nondiffusive transport *Phys. Rev.* E **87** 063106
[64] Mandelbrot B B 1963 The variation of certain speculative prices *J. Bus.* **36** 394
[65] Fama E F 1965 The behaviour of stock market prices *J. Bus.* **38** 34
[66] Mantegna R N and Stanley H E 1995 Scaling behaviour in the dynamics of an economic index *Nature* **376** 46
[67] Frisch U and Frisch H 1995 *Lévy Flights and Related Topics in Physics* (*Lecture Notes in Physics* vol 450) (Springer)
[68] Zumofen G and Klafter J 1995 Absorbing boundary in one-dimensional anomalous transport *Phy. Rev.* E **51** 2805
[69] Chechkin A V, Metzler R, Klafter J, VYu G and Tanatarov L V 2003 First passage and arrival time densities for Lévy flights and the failure of the method of images *J. Phys. A: Math. Gen.* **36** L537
[70] Dybiec B, Gudowska-Nowak E and Chechkin A V 2016 To hit or to pass it over—remarkable transient behaviour of first arrivals and passages for Lévy flights in finite domains *J. Phys. A: Math. Theor.* **49** 504001
[71] Majumdar S N 2010 universal first-passage properties of discrete-time random walks and Lévy flights on a line: statistics of the global maximum and records *Physica* A **389** 4299
[72] Majumdar S N, Mounaix P and Schehr G 2017 Survival probability of random walks and Lévy flights on a semi-infinite line *J. Phys. A: Math. Theor.* **50** 465002
[73] Padash A, Chechkin A V, Dybiec B, Pavlyukevich I, Shokri B and Metzler R 2019 First-passage properties of asymmetric Lévy flights *J. Phys. A: Math. Theor.* **52** 454004
[74] Padash A, Chechkin A V, Dybiec B, Pavlyukevich I, Shokri B and Metzler R 2020 First passage time moments of asymmetric Lévy flights *J. Phys. A: Math. Theor.* **53** 275002
[75] Majumdar S N, Schehr G and Wergen G 2012 Record statistics and persistence for a random walk with a drift *J. Phys. A: Math. Theor.* **45** 355002
[76] Godréche C, Majumdar S N and Schehr G 2017 Record statistics of a strongly correlated time series, random walks and Lévy flights *J. Phys. A: Math. Theor.* **50** 333001

[77] Majumdar S N and Bouchaud J-P 2008 Optimal time to sell a stock in the BlackScholes model: comment on 'Thou Shalt Buy and Hold', by A. Shiryaev, Z. Xu and XY Zhou *Quant. Fin.* **8** 753
[78] Wergen G, Bogner M and Krug J 2011 Record statistics for biased random walks, with an application to financial data *Phys. Rev.* E **83** 051109
[79] Wergen G, Majumdar S N and Schehr G 2012 Record statistics for multiple random walks *Phys. Rev.* E **86** 011119
[80] Mounaix P, Majumdar S N and Schehr G 2018 Asymptotics for the expected maximum of random walks and Lévy flights with a constant drift *J. Stat. Mech.* 083201
[81] Martin R J and Kearney M J 2018 Time since maximum of Brownian motion and asymmetric Lévy processes *J. Phys. A: Math. Theor.* **51** 275001
[82] Heyde C C 1967 A limit theorem for random walks with drift *J. Appl. Probab.* **4** 144
[83] Port S C 1989 Stable processes with drift on the line *Trans. Am. Math. Soc.* **313** 805
[84] Port S C 1990 Asymptotic expansions for the expected volume of a stable sausage *Ann. Probab.* **18** 492
[85] Gikhman I I and Skorokhod A V 1975 *Theory of Stochastic Processes II* (Springer)
[86] Skorokhod A V 1964 *Random Processes With Independent Increments* (Nauka) in Russian
[87] Jespersen S, Metzler R and Fogedby H C 1999 Lévy flights in external force fields: Langevin and fractional Fokker-Planck equations and their solutions *Phys. Rev.* E **59** 2736
[88] Samorodnitsky G and Taqqu M S 1994 *Stable Non-Gaussian Random Processes: Stochastic Models With Infinite Variance* (Chapman and Hall)
[89] Gnedenko B V and Kolmogorov A N 1954 *Limit Distributions for Sums of Random Variables* (Addison-Wesley)
[90] Zolotarev V M 1986 *One-Dimensional Stable Distributions* (American Mathematical Society)
[91] Nolan J P 1997 Numerical calculation of stable densities and distribution functions *Commun. Stat.: Stoch. Models* **13** 759
[92] Fogedby H C 1994 Lévy flights in random environments *Phys. Rev. Lett.* **73** 2517
[93] Fogedby H C 1998 Lévy flights in quenched random force fields *Phys. Rev.* E **58** 1690
[94] Chambers J M, Mallows C L and Stuck B W 1976 A method for simulating stable random variables *J. Am. Stat. Assoc.* **71** 340
[95] Janicki A and Weron A 1994 *Simulation and Chaotic Behavior of α-Stable Stochastic Processes* (Marcel Dekker)
[96] Janicki A 1996 *Numerical and Statistical Approximation of Stochastic Differential Equations With non-Gaussian Measures* (Hugo Steinhaus Centre for Stochastic Methods)
[97] Palyulin V V, Chechkin A V and Metzler R 2014 Space-fractional Fokker-Planck equation and optimization of random search processes in the presence of an external bias *J. Stat. Mech.: Theory Exp.* **11** 11031
[98] Sparre Andersen E 1953 On the fluctuations of sums of random variables *Math. Scand.* **1** 263
[99] Sparre Andersen E 1954 On the fluctuations of sums of random variables II *Math. Scand.* **2** 195
[100] Feller W 1971 *An Introduction to Probability Theory and Its Applications* vol 2 (Wiley)
[101] Chechkin A and Sokolov I M 2018 Random search with resetting: a unified renewal approach *Phys. Rev. Lett.* **121** 050601
[102] Mainardi F 2010 *Fractional Calculus and Waves in Linear Viscoelasticity: An Introduction to Mathematical Models* (Imperial College Press)
[103] Lawley S D 2020 Universal formula for extreme first passage statistics of diffusion *Phys. Rev.* E **101** 012413
[104] Lawley S D 2023 Extreme statistics of superdiffusive Lévy flights and every other Lévy subordinate Brownian motion *J. Nonlinear Sci.* **33** 53
[105] Jia J and Wang H 2015 Fast finite difference methods for space-fractional diffusion equations with fractional derivative boundary conditions *J. Comput. Phys.* **293** 359
[106] Shimin G, Liquan M, Zhengqiang Z and Yutao J 2018 Finite difference/spectral-Galerkin method for a two-dimensional distributed-order time-space fractional reaction-diffusion equation *Appl. Math. Lett.* **85** 157
[107] Deng W H 2008 Finite element method for the space and time fractional Fokker-Planck equation *SIAM J. Numer. Anal.* **47** 204
[108] Melean W and Mustapha K 2007 A second-order accurate numerical method for a fractional wave equation *Numer. Math.* **105** 418
[109] Fix G J and Roop J P 2004 Least squares finite element solution of a fractional order two-point boundary value problem *Comput. Math. Appl.* **48** 1017

[110] Bhrawy A H, Zaky M A and Van Gorder R A 2016 A space-time Legendre spectral tau method for the two-sided space-time Caputo fractional diffusion-wave equation *Numer. Algor.* **71** 151
[111] Li X and Xu C 2009 A space-time spectral method for the time fractional diffusion equation *SIAM J. Numer. Anal.* **47** 2108–31
[112] Odibat Z 2006 Approximations of fractional integrals and Caputo fractional derivatives *Appl. Math. Comput.* **178** 527
[113] Diethelm K and Freed A D 1998 The FracPECE subroutine for the numerical solution of differential equations of fractional order *Forsch. Wissenschaftliches Rechnen* **1999** 57
[114] Podlubny I 1999 *Fractional Differential Equations* (Academic)
[115] Diethelm K, Ford N J and Freed A D 2004 Detailed error analysis for a fractional Adams method *Numer. Algorithms* **36** 31
[116] Kak S 1970 Discrete Hilbert transform *Proc. IEEE* **58** 585